A posteriori error analysis of a momentum conservative Banach-spaces based mixed-FEM for the Navier–Stokes problem *

Jessika Camaño† Sergio Caucao‡
Ricardo Oyarzúa§ Segundo Villa-Fuentes¶

Abstract

In this paper we develop an *a posteriori* error analysis of a new momentum conservative mixed finite element method recently introduced for the steady-state Navier–Stokes problem in two and three dimensions. More precisely, by extending standard techniques commonly used on Hilbert spaces to the case of Banach spaces, such us local estimates, and suitable Helmholtz decompositions, we derive a reliable and efficient residual-based *a posteriori* error estimator for the corresponding mixed finite element scheme on arbitrary (convex or non-convex) polygonal and polyhedral regions. On the other hand, inverse inequalities, the localization technique based on bubble functions, among other tools, are employed to prove the efficiency of the proposed *a posteriori* error indicator. Finally, several numerical results confirming the properties of the estimator and illustrating the performance of the associated adaptive algorithm are reported.

Key words: Navier–Stokes; momentum conservativity; mixed finite element method; Banach spaces; Raviart–Thomas elements; a posteriori; reliability; efficiency

Mathematics Subject Classifications (1991): 65N15, 65N30, 76D05, 76M10

1 Introduction

In this paper we continue the Banach spaces-based study of dual-mixed formulations for nonlinear fluid-flow problems started in [10] (see [7, 11, 17, 16, 19] for recent extensions) by analyzing

*This work was partially supported by CONICYT-Chile through BASAL project CMM, Universidad de Chile, project Fondecyt 1180859, project 77190084 of the PAI Program: Convocatoria Nacional Subvención a la Instalación en la Academia, and the Becas-Chile Programme for Chilean students; and by Universidad del Bío-Bío through VRIP project 194608 GI/C.

†Departamento de Matemática y Física Aplicadas, Universidad Católica de la Santísima Concepción, Casilla 297, Concepción, Chile, and CI^{2}MA, Universidad de Concepción, Casilla 160-C, Concepción, Chile, email: jecamano@ucsc.cl

‡Departamento de Matemática y Física Aplicadas, Universidad Católica de la Santísima Concepción, Casilla 297, Concepción, Chile, email: scaucao@ucsc.cl

§GIMNAP-Departamento de Matemática, Universidad del Bío-Bío, Casilla 5-C, Concepción, Chile, and CI^{2}MA, Universidad de Concepción, Casilla 160-C, Concepción, Chile, email: royarzua@ubiobio.cl.

¶GIMNAP-Departamento de Matemática, Universidad del Bío-Bío, Casilla 5-C, Concepción, Chile, email: segundo.villa1701@alumnos.ubiobio.cl.

a reliable and efficient *a posteriori* error estimator for the momentum conservative mixed finite element method proposed in [10] for the incompressible steady-state Navier–Stokes problem. There, the velocity and a pseudostress tensor, defined in terms of the gradient of the velocity, the pressure and the convective term, are introduced as main unknowns of the system which allows, on the one hand, to preserve exactly conservation of momentum when the datum is in a suitable polynomial space, and on the other hand, to compute other variables of interest, such us the gradient of the velocity and the vorticity, through a simple postprocessing of the pseudostress, tensor, without applying any numerical differentiation, thus avoiding further sources of error. Then, the well-known Banach–Nečas–Babuška theory and the Banach fixed-point theorem are applied to prove the unique solvability of the resulting continuous formulation. Utilizing the same theoretical tools it can be proved that the associated Galerkin scheme defined by Raviart-Thomas elements for the pseudostress and discontinuous piecewise polynomials for the velocity, is well posed.

Now, one of the main tools widely utilized in the numerical analysis community to guarantee a good convergence of most finite element methods, specially under the eventual presence of singularities, is the so called *a posteriori* error estimator. This consists of a global quantity Θ expressed in terms of calculable local indicators Θ_T, defined on each element T of a given triangulation $\mathcal{T}$, which allows to estimate the finite element error in terms of a calculable quantity. This information can be afterwards used to localize sources of error and construct an algorithm to efficiently adapt the mesh. The estimator Θ is said to be efficient (resp. reliable) if there exists $C_1 > 0$ (resp. $C_2 > 0$), independent of the meshsizes, such that

$$C_1 \Theta + \text{h.o.t.} \leq \|\text{error}\| \leq C_2 \Theta + \text{h.o.t.},$$

where h.o.t. is a generic expression denoting one or several terms of higher order.

Going back to our problem of interest, and regarding this powerful tool to improve the performance of numerical methods for partial differential equations, we mention the pioneer works [38], [41] and [42] (se also [4, Section 9.3]) where the authors introduced the first contributions devoted to derive an *a posteriori* error analysis for the incompressible Navier-Stokes problem in its classical velocity-pressure formulation. We refer also to [6] where the authors extend the aforementioned contributions to the case of Dirac measures and [35] for an *a posteriori* error analysis of a Discontinuous Galerkin scheme providing exactly-divergence free approximations of the velocity.

On the other hand, the study of *a posteriori* error estimators for saddle-point problems has been widely developed in the existing literature by many authors (see, e.g. [2], [3], [5], [8], [13], [14], [27], [34], [36], [37], [40], and the references therein). The techniques employed in the above list of contributions have been successfully applied to a quasi-optimal dual-mixed scheme (in [23]) and to augmented-mixed formulations (in [29] and [12], respectively) of the Navier-Stokes problem with constant and variable viscosity.

Our purpose now is to additionally contribute in the direction of the aforementioned works by providing the *a posteriori* error analysis of the mixed variational approach introduced in [10]. To that end, and since our formulation is defined on non-standard Banach spaces, we extend several results usually utilized to analyze *a posteriori* error estimators in Hilbert spaces, to the context of Banach spaces. According to this, the rest of this work is organized as follows. In Section 3 we recall from [10] the model problem and its continuous and discrete fully-mixed variational formulations. Next in Section 4 we provide some preliminary results to be employed next to derive and analyze our *a posteriori* error estimator. The kernel of the present work is given by

Section 5, where we develop the *a posteriori* error analysis. In Section 5.1 we employ the global continuous inf-sup condition, a Helmholtz decomposition, and the local approximation properties of the Clément and Raviart-Thomas operators, to derive a reliable residual-based *a posteriori* error estimator. Then, in Section 5.2 inverse inequalities, and the localization technique based on element-bubble and edge-bubble functions to prove the efficiency of the estimator. Finally, numerical results confirming the reliability and efficiency of the a posteriori error estimator and showing the good performance of the associated adaptive algorithm, are presented in Section 6.

2 Preliminary notations

Let us denote by $\Omega \subseteq \mathbb{R}^d$, $d \in \{2,3\}$ a given bounded domain with polyhedral boundary Γ, and denote by $\mathbf{n}$ the outward unit normal vector on Γ. Standard notations will be adopted for Lebesgue spaces $\mathrm{L}^p(\Omega)$, with $p \in [1,\infty]$ and Sobolev spaces $\mathrm{W}^{r,p}(\Omega)$ with $r \geq 0$, endowed with the norms $\|\cdot\|_{\mathrm{L}^p(\Omega)}$ and $\|\cdot\|_{\mathrm{W}^{r,p}(\Omega)}$, respectively. Note that $\mathrm{W}^{0,p}(\Omega) = \mathrm{L}^p(\Omega)$ and if $p = 2$, we write $\mathrm{H}^r(\Omega)$ in place of $\mathrm{W}^{r,2}(\Omega)$, with the corresponding Lebesgue and Sobolev norms denoted by $\|\cdot\|_{0,\Omega}$ and $\|\cdot\|_{r,\Omega}$, respectively. We also write $|\cdot|_{r,\Omega}$ for the H^r-seminorm. In addition, $\mathrm{H}^{1/2}(\Gamma)$ is the spaces of traces of functions of $\mathrm{H}^1(\Omega)$ and $\mathrm{H}^{-1/2}(\Gamma)$ denotes its dual. With $\langle \cdot, \cdot \rangle_\Gamma$ we denote the corresponding product of duality between $\mathrm{H}^{1/2}(\Gamma)$ and $\mathrm{H}^{-1/2}(\Gamma)$. By $\mathbf{S}$ and $\mathbb{S}$ we will denote the corresponding vectorial and tensorial counterparts of the generic scalar functional space S. In turn, for any vector fields $\mathbf{v} = (v_i)_{i=1,d}$ and $\mathbf{w} = (w_i)_{i=1,d}$ we set the gradient, divergence and tensor product operators, as

$$\nabla \mathbf{v} := \left(\frac{\partial v_i}{\partial x_j}\right)_{i,j=1,d}, \quad \operatorname{div} \mathbf{v} := \sum_{j=1}^{d} \frac{\partial v_j}{\partial x_j}, \quad \text{and} \quad \mathbf{v} \otimes \mathbf{w} := (v_i w_j)_{i,j=1,d}.$$

In addition, for any tensor fields $\boldsymbol{\tau} = (\tau_{ij})_{i,j=1,d}$ and $\boldsymbol{\zeta} = (\zeta_{ij})_{i,j=1,d}$, we let $\mathbf{div}\,\boldsymbol{\tau}$ be the divergence operator div acting along the rows of $\boldsymbol{\tau}$, and define the transpose, the trace, the tensor inner product, and the deviatoric tensor, respectively, as

$$\boldsymbol{\tau}^{\mathrm{t}} := (\boldsymbol{\tau}_{ji})_{i,j=1,d}, \quad \operatorname{tr}(\boldsymbol{\tau}) := \sum_{i=1}^{d} \tau_{ii}, \quad \boldsymbol{\tau} : \boldsymbol{\zeta} := \sum_{i,j=1}^{d} \tau_{ij}\zeta_{ij}, \quad \text{and} \quad \boldsymbol{\tau}^{\mathrm{d}} := \boldsymbol{\tau} - \frac{1}{n}\operatorname{tr}(\boldsymbol{\tau})\mathbb{I},$$

where $\mathbb{I}$ is the identity tensor in $\mathbb{R}^{d\times d}$. For simplicity, in what follows we denote

$$(v,w)_\Omega := \int_\Omega v\,w, \quad (\mathbf{v},\mathbf{w})_\Omega := \int_\Omega \mathbf{v}\cdot\mathbf{w}, \quad (\mathbf{v},\mathbf{w})_\Gamma := \int_\Gamma \mathbf{v}\cdot\mathbf{w} \quad \text{and} \quad (\boldsymbol{\tau},\boldsymbol{\zeta})_\Omega := \int_\Omega \boldsymbol{\tau} : \boldsymbol{\zeta}.$$

Furthermore, we recall that the Hilbert space

$$\mathbf{H}(\operatorname{div};\Omega) := \left\{\tau \in \mathbf{L}^2(\Omega) : \quad \operatorname{div}\tau \in \mathrm{L}^2(\Omega)\right\},$$

equipped with the usual norm $\|\tau\|^2_{\operatorname{div},\Omega} := \|\tau\|^2_{0,\Omega} + \|\operatorname{div}\tau\|^2_{0,\Omega}$ is standard in the realm of mixed problems. However, in the sequel we will make use of the tensor version of $\mathbf{H}(\operatorname{div};\Omega)$, namely

$$\mathbb{H}(\mathbf{div}\,;\Omega) := \left\{\boldsymbol{\tau} \in \mathbb{L}^2(\Omega) : \quad \mathbf{div}\,\boldsymbol{\tau} \in \mathbf{L}^2(\Omega)\right\},$$

whose norm will be denoted $\|\cdot\|_{\mathbf{div},\Omega}$. In turn, given $p > 1$, in what follows we will also employ the non-standard Banach space $\mathbb{H}(\mathbf{div}_p\,;\Omega)$ defined by

$$\mathbb{H}(\mathbf{div}_p\,;\Omega) := \left\{\boldsymbol{\tau} \in \mathbb{L}^2(\Omega) : \quad \mathbf{div}\,\boldsymbol{\tau} \in \mathbf{L}^p(\Omega)\right\},$$

endowed with the norm $\|\boldsymbol{\tau}\|_{\mathbf{div}_p,\Omega} := \left(\|\boldsymbol{\tau}\|^2_{0,\Omega} + \|\mathbf{div}\,\boldsymbol{\tau}\|^2_{\mathbf{L}^p(\Omega)}\right)^{1/2}$.

3 The model problem and its conservative mixed formulation

In this section we recall from [10] the steady-state Navier–Stokes problem, its mixed variational formulation, the associated Galerkin scheme, and the main results concerning the corresponding solvability analysis.

3.1 The steady-state Navier–Stokes problem

Let $\Omega \subseteq \mathbb{R}^d$, $d \in \{2,3\}$ be a bounded domain with Lipschitz boundary Γ and let $\nu > 0$, $\mathbf{u}$ and p be the viscosity, the velocity and pressure, respectively, of a viscous fluid occupying the region Ω, whose movement is described by the incompressible steady-state Navier–Stokes equations with Dirichlet boundary condition:

$$\begin{aligned} -\nu\Delta\mathbf{u} + (\mathbf{u}\cdot\nabla)\mathbf{u} + \nabla p &= \mathbf{f} && \text{in } \Omega, \\ \operatorname{div}\mathbf{u} &= 0 && \text{in } \Omega, \\ \mathbf{u} &= \mathbf{u}_D && \text{on } \Gamma, \\ (p,1)_\Omega &= 0. \end{aligned} \tag{3.1}$$

Above, $\mathbf{f}$ represents an external force acting on Ω and $\mathbf{u}_D$ is the prescribed velocity on Γ, satisfying the compatibility condition:

$$(\mathbf{u}_D\cdot\mathbf{n}, 1)_\Gamma = 0. \tag{3.2}$$

Now, in order to derive our mixed approach (see [10, Section 2.2] for details), we begin by introducing the pseudostress tensor

$$\boldsymbol{\sigma} := \nu\nabla\mathbf{u} \,-\, p\mathbb{I} \,-\, \mathbf{u}\otimes\mathbf{u} \quad \text{in} \quad \Omega.$$

Notice that from the incompressibility condition $\operatorname{tr}(\nabla\mathbf{u}) = \operatorname{div}\mathbf{u} = 0$ in Ω, there hold

$$\mathbf{div}\,(\mathbf{u}\otimes\mathbf{u}) = (\mathbf{u}\cdot\nabla)\mathbf{u} \quad \text{in} \quad \Omega \quad \text{and} \quad \operatorname{tr}(\boldsymbol{\sigma}) = -dp - \operatorname{tr}(\mathbf{u}\otimes\mathbf{u}) \quad \text{in} \quad \Omega.$$

According to the above, we can rewrite equations (3.1), equivalently, as follows

$$\begin{gathered} \boldsymbol{\sigma}^{\mathrm{d}} = \nu\nabla\mathbf{u} - \,(\mathbf{u}\otimes\mathbf{u})^{\mathrm{d}} \quad \text{in} \quad \Omega, \quad -\mathbf{div}\,\boldsymbol{\sigma} \,=\, \mathbf{f} \quad \text{in} \quad \Omega, \\ \mathbf{u} \,=\, \mathbf{u}_D \quad \text{on} \quad \Gamma, \quad (\operatorname{tr}(\boldsymbol{\sigma}),1)_\Omega \,=\, -(\operatorname{tr}(\mathbf{u}\otimes\mathbf{u}),1)_\Omega, \end{gathered} \tag{3.3}$$

where the unknowns of the system are the tensor $\boldsymbol{\sigma}$ and the velocity $\mathbf{u}$. The pressure p can be easily computed as a postprocess of the solution by using

$$p = -\frac{1}{d}(\operatorname{tr}(\boldsymbol{\sigma}) + \operatorname{tr}(\mathbf{u}\otimes\mathbf{u})) \quad \text{in} \quad \Omega.$$

3.2 The mixed variational formulation and its well posedness

In this section we recall from [10, Section 2.3] the weak formulation of (3.3). To that end, we define the spaces $\mathbb{X} := \mathbb{H}(\mathbf{div}_{4/3};\Omega)$, $\mathbf{M} := \mathbf{L}^4(\Omega)$ and

$$\mathbb{X}_0 := \Big\{\boldsymbol{\tau} \in \mathbb{H}(\mathbf{div}_{4/3};\Omega) : \quad (\operatorname{tr}(\boldsymbol{\tau}),1)_\Omega = 0\Big\},$$

and observe that the following decomposition holds:

$$\mathbb{X} = \mathbb{X}_0 \,\oplus\, P_0(\Omega)\mathbb{I},$$

where $P_0(\Omega)$ is the space of constant polynomials on Ω. Then, the variational formulation of (3.3) reads: Find $(\boldsymbol{\sigma}, \mathbf{u}) \in \mathbb{X}_0 \times \mathbf{M}$, such that

$$\begin{aligned} \mathbf{a}(\boldsymbol{\sigma},\boldsymbol{\tau}) \,+\, \mathbf{b}(\boldsymbol{\tau},\mathbf{u}) \,+\, \mathbf{c}(\mathbf{u};\mathbf{u},\boldsymbol{\tau}) \quad &= F(\boldsymbol{\tau}) \quad \forall\, \boldsymbol{\tau} \in \mathbb{X}_0, \\ \mathbf{b}(\boldsymbol{\sigma},\mathbf{v}) \quad &= G(\mathbf{v}) \quad \forall\, \mathbf{v} \in \mathbf{M}, \end{aligned} \tag{3.4}$$

where the bounded forms $\mathbf{a} : \mathbb{X} \times \mathbb{X} \to \mathbb{R}$, $\mathbf{b} : \mathbb{X} \times \mathbf{M} \to \mathbb{R}$ and $\mathbf{c} : \mathbf{M} \times \mathbf{M} \times \mathbb{X} \to \mathbb{R}$ are defined as

$$\mathbf{a}(\boldsymbol{\sigma},\boldsymbol{\tau}) := \frac{1}{\nu}(\boldsymbol{\sigma}^{\mathrm{d}}, \boldsymbol{\tau}^{\mathrm{d}})_\Omega\,, \quad \mathbf{b}(\boldsymbol{\tau},\mathbf{v}) := (\mathbf{div}\ \boldsymbol{\tau}, \mathbf{v})_\Omega, \tag{3.5}$$

and

$$\mathbf{c}(\mathbf{w};\mathbf{v},\boldsymbol{\tau}) := \frac{1}{\nu}(\mathbf{w}\otimes\mathbf{v}, \boldsymbol{\tau}^{\mathrm{d}})_\Omega, \tag{3.6}$$

and the functionals $F \in \mathbb{X}_0'$ and $G \in \mathbf{M}'$ as

$$F(\boldsymbol{\tau}) \,:=\, \langle \boldsymbol{\tau}\mathbf{n}, \mathbf{u}_D\rangle_\Gamma \quad \text{and} \quad G(\mathbf{v}) \,:=\, -(\mathbf{f},\mathbf{v})_\Omega. \tag{3.7}$$

Notice that, from now on, the norms for the spaces $\mathbb{X}$, $\mathbf{M}$ and the product space $\mathbb{X}\times\mathbf{M}$, will be denoted, respectively, by $\|\cdot\|_{\mathbb{X}}$, $\|\cdot\|_{\mathbf{M}}$ and $\|(\cdot,\cdot)\| = \|\cdot\|_{\mathbb{X}} + \|\cdot\|_{\mathbf{M}}$.

This problem is analyzed throughout [10, Section 3], and the well-posedness comes as a result of a fixed-point strategy. In particular, we recall from [10, eq. (3.35)] the following inf-sup condition:

$$\sup_{\substack{(\boldsymbol{\tau},\mathbf{v})\in\mathbb{X}_0\times\mathbf{M} \\ (\boldsymbol{\tau},\mathbf{v})\neq\mathbf{0}}} \frac{\mathbf{a}(\boldsymbol{\zeta},\boldsymbol{\tau}) + \mathbf{b}(\boldsymbol{\tau},\mathbf{z}) + \mathbf{b}(\boldsymbol{\zeta},\mathbf{v}) + \mathbf{c}(\mathbf{u};\mathbf{z},\boldsymbol{\tau})}{\|(\boldsymbol{\tau},\mathbf{v})\|} \geq \frac{\gamma}{2}\|(\boldsymbol{\zeta},\mathbf{z})\| \quad \forall\,(\boldsymbol{\zeta},\mathbf{z}) \in \mathbb{X}_0 \times \mathbf{M}, \tag{3.8}$$

with

$$\gamma := \widetilde{C}\,\frac{\beta\min\{1,\,\nu\beta\}}{\nu\beta+1} \tag{3.9}$$

where $\widetilde{C}$ and β are positive constants independent of the physical parameters. In particular, β is the constant related with the inf-sup condition of the bilinear form b (cf. [10, Lemma 3.4]).

Next, we recall from [10, Theorem 3.7] the well-posedness of (3.4).

Theorem 3.1 *Let* $\mathbf{f} \in \mathbf{L}^{4/3}(\Omega)$ *and* $\mathbf{u}_D \in \mathbf{H}^{1/2}(\Gamma)$ *such that*

$$\frac{4}{\nu\gamma^2}\left(C_F\|\mathbf{u}_D\|_{1/2,\Gamma} \,+\, \|\mathbf{f}\|_{\mathbf{L}^{4/3}(\Omega)}\right) \,<\, 1,$$

where C_F *is the bounding constant of* F *(cf. [10, eq. (3.24)]) and* γ *is defined in* (3.9)*. Then, there exists a unique* $(\boldsymbol{\sigma},\mathbf{u}) \in \mathbb{X}_0 \times \mathbf{M}$ *solution to* (3.4)*. In addition, there exists* $C > 0$*, such that*

$$\|\mathbf{u}\|_{\mathbf{M}} + \|\boldsymbol{\sigma}\|_{\mathbb{X}} \,\leq\, C\left(\|\mathbf{u}_D\|_{1/2,\Gamma} \,+\, \|\mathbf{f}\|_{\mathbf{L}^{4/3}(\Omega)}\right).$$

In particular, it can be proved (see [10, Theorem 3.7]) that the velocity satisfies the following estimate

$$\|\mathbf{u}\|_{\mathbf{M}} \,\leq\, C\left(\|\mathbf{u}_D\|_{1/2,\Gamma} \,+\, \|\mathbf{f}\|_{\mathbf{L}^{4/3}(\Omega)}\right). \tag{3.10}$$

The latter will be employed next in Section 5.1.

We now provide the converse of the derivation of (3.4). More precisely, the following theorem establishes that if $(\boldsymbol{\sigma}, \mathbf{u})$ is the unique solution of (3.4), then $\left(\widetilde{\boldsymbol{\sigma}} := \boldsymbol{\sigma} - \dfrac{1}{d\,|\Omega|}(\mathrm{tr}\,(\mathbf{u}\otimes\mathbf{u}), 1)_\Omega \mathbb{I}, \mathbf{u}\right)$ satisfies (3.3). We remark that there are not extra regularity assumptions on the data; only $\mathbf{f} \in \mathbf{L}^{4/3}(\Omega)$ and $\mathbf{u}_D \in \mathbf{H}^{1/2}(\Gamma)$ are required here.

Theorem 3.2 *Let $(\boldsymbol{\sigma}, \mathbf{u}) \in \mathbb{X}_0 \times \mathbf{M}$ be the unique solution of (3.4). Then, $\boldsymbol{\sigma}^{\mathrm{d}} = \nu\nabla\mathbf{u} - (\mathbf{u}\otimes\mathbf{u})^{\mathrm{d}}$ in Ω, which implies that $\mathbf{u} \in \mathbf{H}^1(\Omega)$, $-\,\mathbf{div}\,\boldsymbol{\sigma} \,=\, \mathbf{f}$ in Ω and $\mathbf{u} \,=\, \mathbf{u}_D$ on Γ.*

Proof. First, it is clear that the identity $-\,\mathbf{div}\,\boldsymbol{\sigma} \,=\, \mathbf{f}$ in Ω follows from the second equation of (3.4). On the other hand, the derivation of the rest of the identities follows from the first equation of (3.4), considering suitable test functions and integrating by parts backwardly. We omit further details. □

3.3 The mixed finite element method

Let $\{\mathcal{T}_h\}_h$ be a family of regular triangulations of $\overline{\Omega}$ by triangles T in $\mathbb{R}^2$ or tetrahedra in $\mathbb{R}^3$ of diameter h_T, such that $\overline{\Omega} = \cup\{T : T \in \mathcal{T}_h\}$ and define $h := \max\{h_T : T \in \mathcal{T}_h\}$. Now, given an integer $l \geq 0$ and a subset S of $\mathbb{R}^d$, we denote by $P_l(S)$ the space of polynomials of total degree at most l defined on S. Hence, for each integer $k \geq 0$ and for each $T \in \mathcal{T}_h$, we define the local Raviart–Thomas space of order k as (see, for instance, [9]):

$$\mathbf{RT}_k(T) := [P_k(T)]^d \oplus \widetilde{P}_k(T)\mathbf{x},$$

where $\mathbf{x} := (x_1, \ldots, x_d)^t$ is a generic vector of $\mathbb{R}^d$ and $\widetilde{P}_k(T)$ is the space of polynomials of total degree equal to k defined on T. In this way, defining the finite element subspaces:

$$\begin{aligned}
\mathbb{X}_h &:= \Big\{\boldsymbol{\tau}_h \in \mathbb{X} : \quad \mathbf{c}^{\mathrm{t}}\boldsymbol{\tau}_h|_T \in \mathbf{RT}_k(T), \quad \forall\,\mathbf{c} \in \mathbb{R}^d, \quad \forall\,T \in \mathcal{T}_h\Big\} \,\subseteq\, \mathbb{X}, \\
\mathbf{M}_h &:= \Big\{\mathbf{v}_h \in \mathbf{M} : \quad \mathbf{v}_h|_T \in [P_k(T)]^d, \quad \forall\,T \in \mathcal{T}_h\Big\} \,\subseteq\, \mathbf{M},
\end{aligned}$$

and observing that

$$\mathbb{X}_h = \mathbb{X}_{h,0} \oplus P_0(\Omega)\mathbb{I} \quad \text{with} \quad \mathbb{X}_{h,0} = \mathbb{X}_h \cap \mathbb{X}_0,$$

the Galerkin scheme associated with problem (3.4) reads: Find $(\boldsymbol{\sigma}_h, \mathbf{u}_h) \in \mathbb{X}_{h,0} \times \mathbf{M}_h$, such that

$$\begin{aligned}
\mathbf{a}(\boldsymbol{\sigma}_h, \boldsymbol{\tau}_h) \,+\, \mathbf{b}(\boldsymbol{\tau}_h, \mathbf{u}_h) \,+\, \mathbf{c}(\mathbf{u}_h; \mathbf{u}_h, \boldsymbol{\tau}_h) \quad &= \, F(\boldsymbol{\tau}_h) \quad \forall\,\boldsymbol{\tau}_h \in \mathbb{X}_{h,0}, \\
\mathbf{b}(\boldsymbol{\sigma}_h, \mathbf{v}_h) \quad &= \, G(\mathbf{v}_h) \quad \forall\,\mathbf{v}_h \in \mathbf{M}_h,
\end{aligned} \tag{3.11}$$

where the forms $\mathbf{a}$, $\mathbf{b}$ and $\mathbf{c}$, as well as the functionals F and G are defined in (3.5), (3.6) and (3.7).

The following results, taken from [10, Theorem 4.5 and Theorem 4.8], respectively, provides the well-posedness of (3.11) and the corresponding theoretical rate of convergence.

Theorem 3.3 *Let* $\mathbf{f} \in \mathbf{L}^{4/3}(\Omega)$ *and* $\mathbf{u}_D \in \mathbf{H}^{1/2}(\Gamma)$ *such that*

$$\frac{4}{\nu\widehat{\gamma}^2}\Big(C_F\|\mathbf{u}_D\|_{1/2,\Gamma} + \|\mathbf{f}\|_{\mathbf{L}^{4/3}(\Omega)}\Big) < 1,$$

where C_F *is the bounding constant of* F*, independent of the physical parameters, and* $\widehat{\gamma}$ *is the discrete version of* γ *(cf.* (3.9)*) given by*

$$\gamma := \widehat{C}\,\frac{\hat{\beta}\min\{1,\,\nu\hat{\beta}\}}{\nu\hat{\beta}+1},$$

where $\widehat{C}$ *is a positive constants independent of the physical parameters and* $\hat{\beta}$ *is the constant related with the discrete inf-sup condition of the bilinear form* b*. Then, there exists a unique* $(\boldsymbol{\sigma}_h, \mathbf{u}_h) \in \mathbb{X}_{h,0} \times \mathbf{M}_h$ *solution to* (3.11)*. In addition, there exists* $C > 0$*, independent of* h*, such that*

$$\|\mathbf{u}_h\|_{\mathbf{M}} + \|\boldsymbol{\sigma}_h\|_{\mathbb{X}} \le C\Big(\|\mathbf{u}_D\|_{1/2,\Gamma} + \|\mathbf{f}\|_{\mathbf{L}^{4/3}(\Omega)}\Big).$$

In particular, it can be proved (see [10, Theorem 3.7]) that the discrete velocity satisfies the following estimate

$$\|\mathbf{u}_h\|_{\mathbf{M}} \le C\Big(\|\mathbf{u}_D\|_{1/2,\Gamma} + \|\mathbf{f}\|_{\mathbf{L}^{4/3}(\Omega)}\Big). \tag{3.12}$$

The latter will be employed next in Section 5.1.

Theorem 3.4 *Assume that*

$$\frac{4}{\nu\gamma\widehat{\gamma}}\Big(C_F\|\mathbf{u}_D\|_{1/2,\Gamma} + \|\mathbf{f}\|_{\mathbf{L}^{4/3}(\Omega)}\Big) \le \frac{1}{2},$$

being C_F *the bounding constant of* F *(cf. [10, eq. (3.24)]),* γ *defined in* (3.9) *and* $\widehat{\gamma}$ *the discrete version of* γ *(cf. [10, eq. (4.21)]). In addition, let* $(\boldsymbol{\sigma}, \mathbf{u}) \in \mathbb{X}_0 \times \mathbf{M}$ *and* $(\boldsymbol{\sigma}_h, \mathbf{u}_h) \in \mathbb{X}_{h,0} \times \mathbf{M}_h$ *be the unique solutions of problems* (3.4) *and* (3.11)*, respectively. and assume further that* $\boldsymbol{\sigma} \in \mathbb{H}^{l+1}(\Omega)$*,* $\mathbf{div}\,\boldsymbol{\sigma} \in \mathbf{W}^{l+1,4/3}(\Omega)$ *and* $\mathbf{u} \in \mathbf{W}^{l+1,4}(\Omega)$*, for* $0 \le l \le k$*. Then, there exists* $C > 0$*, independent of* h*, such that*

$$\|(\boldsymbol{\sigma} - \boldsymbol{\sigma}_h, \mathbf{u} - \mathbf{u}_h)\| \le C\,h^{l+1}\Big\{|\boldsymbol{\sigma}|_{\mathbb{H}^{l+1}(\Omega)} + |\mathbf{div}\,\boldsymbol{\sigma}|_{\mathbf{W}^{l+1,4/3}(\Omega)} + |\mathbf{u}|_{\mathbf{W}^{l+1,4}(\Omega)}\Big\}.$$

4 Preliminary results for the a posteriori error analysis

We start by introducing some useful notations to describe local information on elements and edges or faces depending if $d = 2$ or $d = 3$, respectively. Let $\mathcal{E}_h$ be the set of edges or faces of $\mathcal{T}_h$, whose corresponding diameters are denoted h_e, and define

$$\mathcal{E}_h(\Omega) := \big\{ e \in \mathcal{E}_h : \quad e \subseteq \Omega \big\} \quad \text{and} \quad \mathcal{E}_h(\Gamma) := \big\{ e \in \mathcal{E}_h : \quad e \subseteq \Gamma \big\}.$$

For each $T \in \mathcal{T}_h$, we let $\mathcal{E}_{h,T}$ be the set of edges or faces of T, and we denote

$$\mathcal{E}_{h,T}(\Omega) = \big\{ e \subseteq \partial T : \quad e \in \mathcal{E}_h(\Omega) \big\} \quad \text{and} \quad \mathcal{E}_{h,T}(\Gamma) = \big\{ e \subseteq \partial T : \quad e \in \mathcal{E}_h(\Gamma) \big\}.$$

We also define unit normal vector $\mathbf{n}_e$ on each edge or face by

$$\mathbf{n}_e := (n_1, .., n_d)^{\mathrm{t}} \quad \forall\, e \in \mathcal{E}_h.$$

Hence, when $d = 2$, we can define the tangential vector $\boldsymbol{s}_e$ by

$$\boldsymbol{s}_e := (-n_2, n_1)^{\mathrm{t}} \quad \forall\, e \in \mathcal{E}_h\,.$$

However, when no confusion arises, we will simply write $\mathbf{n}$ and $\boldsymbol{s}$ instead of $\mathbf{n}_e$ and $\boldsymbol{s}_e$, respectively.

The usual jump operator $[\![\cdot]\!]$ across internal edges or face are defined for piecewise continuous matrix, vector, or scalar-valued functions $\boldsymbol{\zeta}$ by

$$[\![\boldsymbol{\zeta}]\!] = (\boldsymbol{\zeta}\big|_{T_+})\big|_e - (\boldsymbol{\zeta}\big|_{T_-})\big|_e \quad \text{with} \quad e = \partial T_+ \cap \partial T_-,$$

where T_+ and T_- are the elements of $\mathcal{T}_h$ having e as a common edge or face. Finally, for sufficiently smooth scalar ψ, vector $\mathbf{v} := (v_1, .., v_d)^{\mathrm{t}}$, and tensor fields $\boldsymbol{\tau} := (\tau_{ij})_{1\le i,j\le d}$, for $d = 2$ we let

$$\operatorname{curl}(\psi) := \Big(\frac{\partial\psi}{\partial x_2}, -\frac{\partial\psi}{\partial x_1}\Big)^{\mathrm{t}}, \quad \operatorname{rot}(\mathbf{v}) := \frac{\partial \mathbf{v}_2}{\partial x_1} - \frac{\partial \mathbf{v}_1}{\partial x_2}, \quad \mathbf{curl}(\mathbf{v}) = \begin{pmatrix} \operatorname{curl}(v_1)^{\mathrm{t}} \\ \operatorname{curl}(v_2)^{\mathrm{t}} \end{pmatrix},$$

$$\underline{\mathbf{curl}}(\boldsymbol{\tau}) = \begin{pmatrix} \operatorname{rot}(\boldsymbol{\tau}_1) \\ \operatorname{rot}(\boldsymbol{\tau}_2) \end{pmatrix} \quad \text{and} \quad \boldsymbol{\gamma}_*(\boldsymbol{\tau}) = \boldsymbol{\tau}\boldsymbol{s}$$

and for $d = 3$ we let

$$\mathbf{curl}(\mathbf{v}) = \nabla \times \mathbf{v}\,, \quad \underline{\mathbf{curl}}(\boldsymbol{\tau}) = \begin{pmatrix} \mathbf{curl}(\boldsymbol{\tau}_1) \\ \mathbf{curl}(\boldsymbol{\tau}_2) \\ \mathbf{curl}(\boldsymbol{\tau}_3) \end{pmatrix} \quad \text{and} \quad \boldsymbol{\gamma}_*(\boldsymbol{\tau}) = \begin{pmatrix} \boldsymbol{\tau}_1 \times \mathbf{n} \\ \boldsymbol{\tau}_2 \times \mathbf{n} \\ \boldsymbol{\tau}_3 \times \mathbf{n} \end{pmatrix},$$

where $\boldsymbol{\tau}_i$ is the $i-$th row of $\boldsymbol{\tau}$ and the derivatives involved are taken in the distributional sense.

Let us now recall the main properties of the Raviart–Thomas interpolator (see e.g. [22]) and the Clément operator (see e.g. [18]) onto the space of continuous piecewise linear functions. Given $p > 1$, let us define the space

$$\mathbf{Z}_p := \big\{\tau \in \mathbf{H}(\mathrm{div}_p;\Omega) : \quad \tau|_T \in \mathbf{W}^{1,p}(T), \quad \forall\, T \in \mathcal{T}_h\big\},$$

and let

$$\Pi_h^k : \mathbf{Z}_p \to \mathbf{X}_h := \big\{\tau \in \mathbf{H}(\mathrm{div};\Omega) : \quad \tau|_T \in \mathbf{RT}_k(T), \quad \forall\, T \in \mathcal{T}_h\big\},$$

be the Raviart–Thomas interpolation operator, which is well defined in $\mathbf{Z}_p$ (see e.g. [22, Section 1.2.7]) and is characterized by the identities

$$(\Pi_h^k(\tau)\cdot\mathbf{n}, \xi)_e = (\tau\cdot\mathbf{n}, \xi)_e \quad \forall\, \xi \in P_k(e),\ \forall \text{ edge or face } e \text{ of } \mathcal{T}_h, \tag{4.1}$$

and

$$(\Pi_h^k(\tau), \psi)_T = (\tau, \psi)_T \quad \forall\, \psi \in [P_{k-1}(T)]^d,\ \forall\, T \in \mathcal{T}_h \ (\text{if } k \ge 1)\,.$$

Notice that, since $\Pi_h^k(\tau)\cdot\mathbf{n}_e \in P_k(e)$, from (4.1) we have that

$$\Pi_h^k(\tau)\cdot\mathbf{n}_e = \mathcal{P}_e^k(\tau\cdot\mathbf{n}_e)\,, \tag{4.2}$$

where, for $1 \le r \le \infty$, $\mathcal{P}_e^k : L^r(e) \to P_k(e)$ is the operator satisfying

$$\int_e (\mathcal{P}_e^k(v) - v) z_h = 0 \quad \forall\, z_h \in P_k(e), \tag{4.3}$$

Notice that for $r = 2$, $\mathcal{P}_e^k$ coincides with the usual orthogonal projection. In addition, it is well known (see e.g. [22, Lemma 1.41]) that the following identity holds

$$\mathrm{div}(\Pi_h^k(\tau)) = \mathcal{P}_h^k(\mathrm{div}\tau) \quad \forall\, \tau \in \mathbf{Z}_p,$$

where, given $1 \leq r \leq \infty$, $\mathcal{P}_h^k : L^r(\Omega) \to M_h := \left\{ v \in \mathrm{L}^2(\Omega) : \quad v|_T \in P_k(T) \quad \forall\, T \in \mathcal{T}_h \right\}$ is the operator satisfying

$$\int_\Omega (\mathcal{P}_h^l(v) - v) z_h = 0 \quad \forall\, z_h \in M_h.$$

The following lemma establishes the local approximation properties of Π_h^k.

Lemma 4.1 *Let $p > 1$. Then, there exists $c_1 > 0$, independent of h, such that for each $\tau \in \mathbf{W}^{l+1,p}(T)$ with $0 \leq l \leq k$, and for each $0 \leq m \leq l+1$, there holds*

$$|\tau - \Pi_h^k(\tau)|_{\mathbf{W}^{m,p}(T)} \leq c_1 \frac{h_T^{l+2}}{\rho_T^{m+1}} |\tau|_{\mathbf{W}^{l+1,p}(T)},$$

where ρ_T is the diameter of the largest sphere contained in T. Moreover, there exists $c_2 > 0$, independent of h, such that for each $\tau \in \mathbf{W}^{1,p}(T)$, with $\mathrm{div}\,\tau \in \mathrm{W}^{l+1,p}(T)$ and $0 \leq l \leq k$, and for each $0 \leq m \leq l+1$, there holds

$$|\mathrm{div}\,\tau - \mathrm{div}\,(\Pi_h^k(\tau))|_{\mathrm{W}^{m,p}(T)} \leq c_2 \frac{h_T^{l+1}}{\rho_T^{m}} |\mathrm{div}\,\tau|_{\mathrm{W}^{l+1,p}(T)}.$$

Proof. See [10, Lemma 4.2] for details. □

Now, before introducing the following lemma, let us now recall some classical notation and results. Let $\widehat{T}$ be a fixed reference element, which usually corresponds to the triangle with vertices (1, 0), (0, 1), and (0, 0) in $\mathbb{R}^2$, or the tetrahedron with vertices (1, 0, 0), (0, 1, 0), (0, 0, 1), and (0, 0, 0) in $\mathbb{R}^3$. Any $T \in \mathcal{T}_h$ can be obtained by mapping $\widehat{T}$ using an affine map. By this we mean that for any $T \in \mathcal{T}_h$ there is a map $F_T : \widehat{T} \to T$ such that $F_T(\widehat{T}) = T$ and $F_T(\widehat{x}) = B_T\widehat{x} + b_T$ where $B_T \in \mathbb{R}^d \times \mathbb{R}^d$ is an invertible matrix and b_T is a vector in $\mathbb{R}^d$.

Given $T \in \mathcal{T}_h$ and $e \in \mathcal{E}_{h,T}$, we let $\widehat{e}$ be the face or edge of $\widehat{T}$ satisfying $e = F_T(\widehat{e})$. Then, the following change of variable formula holds

$$(f, 1)_e = \frac{|e|}{|\widehat{e}|}(f \circ F_T, 1)_{\widehat{e}} = \frac{|e|}{|\widehat{e}|}(\widehat{f}, 1)_{\widehat{e}}. \tag{4.4}$$

It is easy to prove that

$$\widehat{\mathcal{P}_e^k(v)} = \mathcal{P}_{\widehat{e}}^k(\widehat{v}) \tag{4.5}$$

where, for $1 \leq r \leq \infty$, $\mathcal{P}_{\widehat{e}}^k : L^r(\widehat{e}) \to P_k(\widehat{e})$ is defined as in (4.3).

Finally, let $\boldsymbol{\mathcal{P}}_{\widehat{T}}^k : \mathbf{L}^2(\widehat{T}) \to \mathbf{P}_k(\widehat{T})$ be the usual orthogonal projector and $\mathbf{n}_{\widehat{e}}$ the unit normal vector on $\widehat{e}$. Notice that

$$\boldsymbol{\mathcal{P}}_{\widehat{T}}^k(\widehat{\tau}) \cdot \mathbf{n}_{\widehat{e}}|_{\widehat{e}} \in P_k(\widehat{e}). \tag{4.6}$$

Now we are in position of presenting the following lemma which extends the approximation property of the Raviart–Thomas operator on edges or faces, originally given for Hilbert spaces (cf. G.N. Gatica, 2019, private communication).

Lemma 4.2 *Let $p > 1$, $T \in \mathcal{T}_h$ and $e \in \mathcal{E}_{h,T}$. Then, there exists $C > 0$, independent of h, such that*

$$\|\tau \cdot \mathbf{n} - \Pi_h^k(\tau) \cdot \mathbf{n}\|_{\mathrm{L}^p(e)} \,\leq\, C h_e^{1-1/p} |\tau|_{\mathbf{W}^{1,p}(T)} \qquad \forall\, \tau \in \mathbf{W}^{1,p}(T). \tag{4.7}$$

Proof. We begin by proceeding similarly as in [25, Lemma 3.18]. In fact, given $T \in \mathcal{T}_h$ and $e \in \mathcal{E}_{h,T}$, we let $\widehat{e} \in \mathcal{E}_{h,\widehat{T}}$, be such that $e = F_T(\widehat{e})$. Then, given $\tau \in \mathbf{W}^{1,p}(T)$, from (4.2), the identities (4.4) and (4.5), and the property (4.6), we obtain

$$\|\tau \cdot \mathbf{n}_e - \Pi_h^k(\tau) \cdot \mathbf{n}_e\|_{\mathrm{L}^p(e)} \leq \frac{|e|^{1/p}}{|\widehat{e}|^{1/p}} \|\widehat{\tau \cdot \mathbf{n}} - \mathcal{P}_{\widehat{e}}^k(\widehat{\tau \cdot \mathbf{n}})\|_{\mathrm{L}^p(\widehat{e})} \leq \frac{|e|^{1/p}}{|\widehat{e}|^{1/p}} \|\widehat{\tau} \cdot \mathbf{n}_{\widehat{e}} - \boldsymbol{\mathcal{P}}_{\widehat{T}}^k(\widehat{\tau}) \cdot \mathbf{n}_{\widehat{e}}\|_{\mathrm{L}^p(\widehat{e})}. \tag{4.8}$$

Then, making use of the Rellich–Kondrachov Theorem (see [22, Theorem B.46]) with $s = 1/p'$ being p' the real number satisfying $1/p + 1/p' = 1$, $\Omega = \widehat{e}$, and the trace theorem in $\mathbf{W}^{1,p}(\widehat{T})$ (see, for instance, [31, Theorem 1.5.1.3]), we obtain

$$\|\widehat{\tau} \cdot \mathbf{n}_{\widehat{e}} - \boldsymbol{\mathcal{P}}_{\widehat{T}}^k(\widehat{\tau}) \cdot \mathbf{n}_{\widehat{e}}\|_{\mathrm{L}^p(\widehat{e})} \quad \leq \widehat{c}\, \|\widehat{\tau} - \boldsymbol{\mathcal{P}}_{\widehat{T}}^k(\widehat{\tau})\|_{\mathrm{W}^{1/p',p}(\widehat{e})} \leq \widehat{C}\, \|\widehat{\tau} - \boldsymbol{\mathcal{P}}_{\widehat{T}}^k(\widehat{\tau})\|_{\mathbf{W}^{1,p}(\widehat{T})}. \tag{4.9}$$

Next, since $\boldsymbol{\mathcal{P}}_{\widehat{T}}^k \in \mathcal{L}(\mathbf{W}^{1,p}(\widehat{T}), \mathbf{W}^{1,p}(\widehat{T}))$ and $\boldsymbol{\mathcal{P}}_{\widehat{T}}^k(\widehat{\mathbf{q}}) = \widehat{\mathbf{q}}$ for all $\widehat{\mathbf{q}} \in \mathbf{P}_k(\widehat{T})$, we can apply the L^p-version of the Deny–Lions and Bramble–Hilbert lemmas (see, for instance, [22, Lemma B.67] and [22, Lemma B.68], respectively) to $\boldsymbol{\mathcal{P}}_{\widehat{T}}^k$, obtaining

$$\|\widehat{\tau} - \boldsymbol{\mathcal{P}}_{\widehat{T}}^k(\widehat{\tau})\|_{\mathbf{W}^{1,p}(\widehat{T})} \leq \hat{C} |\widehat{\tau}|_{\mathbf{W}^{1,p}(\widehat{T})}. \tag{4.10}$$

Now, employing the scaling estimate in [22, Lemma 1.101], geometric results (see, for instance, [22, Lemma 1.100]) and the fact that $|T| \cong h_T^d$ and $h_e \cong h_T$, the latter obtained thanks to the fact that we are considering a regular triangulation, we deduce that

$$|\widehat{\tau}|_{\mathbf{W}^{1,p}(\widehat{T})} \quad \leq \widetilde{C} \|B_T\| \,|\det(B_T)|^{-1/p} |\tau|_{\mathbf{W}^{1,p}(T)} \leq C h_e^{1-d/p} |\boldsymbol{\tau}|_{\mathbf{W}^{1,p}(T)},$$

which, together with (4.8), (4.9), (4.10) and the fact that $|e| \cong h_e^{d-1}$ completes the proof. $\square$

Let us consider now the space $\mathrm{H}_h^1 = \big\{ v_h \in \mathrm{C}(\bar{\Omega}) : \quad v_h\big|_T \in P_1(T) \quad \forall\, T \in \mathcal{T}_h \big\}$. Then, we denote by $I_h : \mathrm{H}^1(\Omega) \longrightarrow \mathrm{H}_h^1$ the well known Clément interpolation operator. The local approximation properties of this operator are established in the following lemma (see [18]):

Lemma 4.3 *There exist constants c_1, $c_2 > 0$, independent of h, such that for all $v \in \mathrm{H}^1(\Omega)$ there holds*

$$\|v \,-\, I_h v\|_{0,T} \,\leq\, c_1\, h_T\, |v|_{1,\Delta(T)} \quad \forall\, T \in \mathcal{T}_h,$$

and

$$\|v \,-\, I_h v\|_{0,e} \,\leq\, c_2\, h_e^{1/2}\, \|v\|_{1,\Delta(e)} \quad \forall\, e \in \mathcal{E}_h,$$

where $\Delta(T)$ and $\Delta(e)$ are the set of elements intersecting T and e, respectively.

In what follows we will employ a tensor version of Π_h^k, denoted by $\boldsymbol{\Pi}_h^k : \mathbb{Z}_p \to \mathbb{X}$, which is defined row-wise by Π_h^k and the vector version of I_h, denote by $\mathbf{I}_h : \mathbf{H}^1(\Omega) \to \mathbf{H}_h^1$, defined component-wise by I_h.

We end this section by establishing a suitable Helmholtz decomposition for $\mathbb{H}(\mathbf{div}_p\,; \Omega)$.

Lemma 4.4 *Let $p > 1$. Then, for each $\boldsymbol{\tau} \in \mathbb{H}(\mathbf{div}_p, \Omega)$ there exist*

a) $\boldsymbol{\xi} \in \mathbb{W}^{1,p}(\Omega)$ *and* $\mathbf{w} \in \mathbf{H}^1(\Omega)$ *such that* $\boldsymbol{\tau} = \boldsymbol{\xi} + \mathbf{curl}\, \mathbf{w}$ *when* $d = 2$,

b) $\boldsymbol{\xi} \in \mathbb{W}^{1,p}(\Omega)$ *and* $\mathbf{w} \in \mathbb{H}^1(\Omega)$ *such that* $\boldsymbol{\tau} = \boldsymbol{\xi} + \underline{\mathbf{curl}}\, \mathbf{w}$ *when* $d = 3$.

In addition, in both cases,

$$\|\boldsymbol{\xi}\|_{\mathbb{W}^{1,p}(\Omega)} + \|\mathbf{w}\|_{1,\Omega} \leq C_{Hel} \|\boldsymbol{\tau}\|_{\mathbf{div}_p,\Omega}, \tag{4.11}$$

where C_{Hel} is a positive constant independent of all the foregoing variables.

Proof. In what follows we prove the result for the two-dimensional case. The three-dimensional case can be treated similarly by extending [24, Theorem 3.1] to the L^p case.

Let B a bounded convex polygonal domain containing $\overline{\Omega}$. Then, given $\boldsymbol{\tau} \in \mathbb{H}(\mathbf{div}_p; \Omega)$ we let $\mathbf{z} \in \mathbf{W}_0^{1,p}(B)$ be the unique weak solution of the boundary value problem:

$$\Delta \mathbf{z} = \mathbf{div}\, \boldsymbol{\tau} \quad \text{in} \quad \Omega, \qquad \Delta \mathbf{z} = \mathbf{0} \quad \text{in} \quad B \setminus \Omega, \qquad \mathbf{z} = \mathbf{0} \quad \text{on} \quad \partial B,$$

which, owing to the fact that B is convex, belongs to $\mathbf{W}^{2,p}(B)$ and satisfies (see for instance [31, Theorem 2.4.2.5]):

$$\|\mathbf{z}\|_{\mathbf{W}^{2,p}(\Omega)} \leq \|\mathbf{z}\|_{\mathbf{W}^{2,p}(B)} \leq \|\mathbf{div}\, \boldsymbol{\tau}\|_{\mathbf{L}^p(\Omega)}.$$

Then, we set $\boldsymbol{\xi} = (\nabla \mathbf{z})|_\Omega \in \mathbb{W}^{1,p}(\Omega)$ which clearly satisfies $\mathbf{div}\, \boldsymbol{\xi} = \Delta \mathbf{z} = \mathbf{div}\, \boldsymbol{\tau}$ in Ω and

$$\|\boldsymbol{\xi}\|_{\mathbb{W}^{1,p}(\Omega)} \leq \|\mathbf{div}\, \boldsymbol{\tau}\|_{\mathbf{L}^p(\Omega)}. \tag{4.12}$$

Now, let $\boldsymbol{\varepsilon} := \boldsymbol{\tau} - \boldsymbol{\xi}$ and observe that $\mathbf{div}\, \boldsymbol{\varepsilon} = \mathbf{0}$ in Ω. In addition, thanks to the continuous embedding $W^{1,p}(\Omega)$ into $L^2(\Omega)$ (see, for instance, [22, Theorem B.46]) and (4.12) we obtain that $\boldsymbol{\varepsilon} \in \mathbb{L}^2(\Omega)$ and

$$\|\boldsymbol{\varepsilon}\|_{0,\Omega} \leq \widehat{c} \left(\|\boldsymbol{\tau}\|_{0,\Omega} + \|\boldsymbol{\xi}\|_{\mathbb{W}^{1,p}(\Omega)} \right) \leq \widetilde{c} \|\boldsymbol{\tau}\|_{\mathbf{div}_p,\Omega}.$$

In this way, since Ω is connected and $\boldsymbol{\varepsilon} \in \mathbb{L}^2(\Omega)$ satisfies $\mathbf{div}\, \boldsymbol{\varepsilon} = \mathbf{0}$ in Ω, from [30, Chapter I, Theorem 3.1] we conclude that there exists $\mathbf{w} = (w_1, w_2)^{\mathrm{t}} \in \mathbf{H}^1(\Omega)$, such that

$$\boldsymbol{\varepsilon} = \boldsymbol{\tau} - \boldsymbol{\xi} = \mathbf{curl}\, \mathbf{w} \quad \text{in} \quad \Omega, \tag{4.13}$$

which can be chosen so that $(w_1, 1)_\Omega = (w_2, 1)_\Omega = 0$. In turn, the equivalence between $\|\mathbf{w}\|_{1,\Omega}$ and $|\mathbf{w}|_{1,\Omega}$, together with (4.12) (4.13) and the continuous embedding from $W^{1,p}(\Omega)$ into $L^2(\Omega)$, imply

$$\|\mathbf{w}\|_{1,\Omega} \leq c |\mathbf{w}|_{1,\Omega} = c \|\mathbf{curl}\, \mathbf{w}\|_{0,\Omega} \leq c (\|\boldsymbol{\tau}\|_{0,\Omega} + \|\boldsymbol{\xi}\|_{\mathbb{W}^{1,p}(\Omega)}) \leq c \|\boldsymbol{\tau}\|_{\mathbf{div}_p,\Omega}.$$

Finally, the foregoing inequality and (4.12) confirm the stability estimate (4.11), thus finishing the proof. □

5 A posteriori error analysis

In this section we derive a residual-based *a posteriori* error estimator for the mixed method (3.11). To that end, in what follows we assume that the hypothesis of Theorems 3.1 and 3.3 hold and let $(\boldsymbol{\sigma}, \mathbf{u}) \in \mathbb{X}_0 \times \mathbf{M}$ and $(\boldsymbol{\sigma}_h, \mathbf{u}_h) \in \mathbb{X}_{h,0} \times \mathbf{M}_h$ be the unique solutions of the continuous and discrete problems (3.4) and (3.11), respectively. Then, our global *a posteriori* error estimator is defined by:

$$\Theta = \left\{ \sum_{T \in \mathcal{T}_h} \Theta_T^2 \right\}^{1/2} + \left\{ \sum_{T \in \mathcal{T}_h} \|\mathbf{f} + \mathbf{div}\, \boldsymbol{\sigma}_h\|_{\mathbf{L}^{4/3}(T)}^{4/3} \right\}^{3/4} \tag{5.1}$$

where, for each $T \in \mathcal{T}_h$, the local error indicator is defined as follows:

$$\begin{aligned}\Theta_T^2 := h_T^{2-d/2} \left\| \nabla \mathbf{u}_h - \frac{1}{\nu}(\boldsymbol{\sigma}_h + (\mathbf{u}_h \otimes \mathbf{u}_h))^{\mathrm{d}} \right\|_{0,T}^2 + \sum_{e \in \mathcal{E}_{h,T}(\Gamma)} h_e^{1/2}\, \|\mathbf{u}_D - \mathbf{u}_h\|_{\mathbf{L}^4(e)}^2 \\ + h_T^2 \left\| \underline{\mathbf{curl}} \left(\frac{1}{\nu}(\boldsymbol{\sigma}_h + (\mathbf{u}_h \otimes \mathbf{u}_h))^{\mathrm{d}} \right) \right\|_{0,T}^2 + \sum_{e \in \mathcal{E}_{h,T}(\Omega)} h_e \left\| \left[\!\left[\boldsymbol{\gamma}_* \left(\frac{1}{\nu}(\boldsymbol{\sigma}_h + (\mathbf{u}_h \otimes \mathbf{u}_h))^{\mathrm{d}} \right) \right]\!\right] \right\|_{0,e}^2 \\ + \sum_{e \in \mathcal{E}_{h,T}(\Gamma)} h_e \left\| \boldsymbol{\gamma}_* \left(\frac{1}{\nu}(\boldsymbol{\sigma}_h + (\mathbf{u}_h \otimes \mathbf{u}_h))^{\mathrm{d}} - \nabla \mathbf{u}_D \right) \right\|_{0,e}^2 .\end{aligned} \tag{5.2}$$

The main goal of the present section is to establish, under suitable assumptions, We begin with the reliability of the estimator.

5.1 Reliability of the a posteriori error estimator

The main result of this section is stated in the following theorem.

Theorem 5.1 *Assume that the data* $\mathbf{f}$ *and* $\mathbf{u}_D$ *satisfy*

$$\frac{8}{\nu \gamma \widehat{\gamma}} \left(C_F \|\mathbf{u}_D\|_{1/2,\Gamma} + \|\mathbf{f}\|_{\mathbf{L}^{4/3}(\Omega)} \right) \leq 1. \tag{5.3}$$

Then, there exist $C_{rel} > 0$*, independent of* h*, such that*

$$\|(\boldsymbol{\sigma} - \boldsymbol{\sigma}_h, \mathbf{u} - \mathbf{u}_h)\| \leq C_{rel}\, \Theta. \tag{5.4}$$

We begin the derivation of (5.4) with the next preliminary lemma.

Lemma 5.2 *Assume that the data* $\mathbf{f}$ *and* $\mathbf{u}_D$ *satisfy* (5.3)*. Let* $(\boldsymbol{\sigma}, \mathbf{u}) \in \mathbb{X}_0 \times \mathbf{M}$ *and* $(\boldsymbol{\sigma}_h, \mathbf{u}_h) \in \mathbb{X}_{h,0} \times \mathbf{M}_h$ *solution to* (3.4) *and* (3.11)*, respectively. Then, there exists a constant* $C_{glob} > 0$*, independent of* h*, such that*

$$\|(\boldsymbol{\sigma} - \boldsymbol{\sigma}_h, \mathbf{u} - \mathbf{u}_h)\| \;\leq\; C_{glob} \sup_{\substack{(\boldsymbol{\tau}, \mathbf{v}) \in \mathbb{X}_0 \times \mathbf{M} \\ (\boldsymbol{\tau}, \mathbf{v}) \neq \mathbf{0}}} \frac{\mathcal{R}(\boldsymbol{\tau}, \mathbf{v})}{\|(\boldsymbol{\tau}, \mathbf{v})\|}, \tag{5.5}$$

where $\mathcal{R} : \mathbb{X}_0 \times \mathbf{M} \to \mathbb{R}$ *is the residual functional*

$$\mathcal{R}(\boldsymbol{\tau}, \mathbf{v}) = \mathbf{a}(\boldsymbol{\sigma} - \boldsymbol{\sigma}_h, \boldsymbol{\tau}) + \mathbf{b}(\boldsymbol{\tau}, \mathbf{u} - \mathbf{u}_h) + \mathbf{b}(\boldsymbol{\sigma} - \boldsymbol{\sigma}_h, \mathbf{v}) + \mathbf{c}(\mathbf{u}; \mathbf{u}, \boldsymbol{\tau}) - \mathbf{c}(\mathbf{u}_h; \mathbf{u}_h, \boldsymbol{\tau}) \tag{5.6}$$

for all $(\boldsymbol{\tau}, \mathbf{v}) \in \mathbb{X}_0 \times \mathbf{M}$.

Proof. First, using the inf-sup condition (3.8) for the error $(\boldsymbol{\zeta}, \mathbf{z}) = (\boldsymbol{\sigma} - \boldsymbol{\sigma}_h, \mathbf{u} - \mathbf{u}_h)$, adding and substracting suitable terms, using the notation introduced in (5.6), and the fact that

$$|\mathbf{c}(\mathbf{u} - \mathbf{u}_h; \mathbf{u}_h, \boldsymbol{\tau})| \leq \frac{1}{\nu} \|\mathbf{u}_h\|_{\mathbf{M}} \|\mathbf{u} - \mathbf{u}_h\|_{\mathbf{M}} \|\boldsymbol{\tau}\|_{\mathbb{X}},$$

it follows that

$$\begin{aligned}
\frac{\gamma}{2} \|(\boldsymbol{\sigma} - \boldsymbol{\sigma}_h, \mathbf{u} - \mathbf{u}_h)\| \;&\leq \sup_{\substack{(\boldsymbol{\tau}, \mathbf{v}) \in \mathbb{X}_0 \times \mathbf{M} \\ (\boldsymbol{\tau}, \mathbf{v}) \neq \mathbf{0}}} \frac{\mathcal{R}(\boldsymbol{\tau}, \mathbf{v})}{\|(\boldsymbol{\tau}, \mathbf{v})\|} + \sup_{\substack{\boldsymbol{\tau} \in \mathbb{X}_0 \\ \boldsymbol{\tau} \neq \mathbf{0}}} \frac{\mathbf{c}(\mathbf{u} - \mathbf{u}_h; \mathbf{u}_h, \boldsymbol{\tau})}{\|\boldsymbol{\tau}\|_{\mathbb{X}}} \\
&\leq \sup_{\substack{(\boldsymbol{\tau}, \mathbf{v}) \in \mathbb{X}_0 \times \mathbf{M} \\ (\boldsymbol{\tau}, \mathbf{v}) \neq \mathbf{0}}} \frac{\mathcal{R}(\boldsymbol{\tau}, \mathbf{v})}{\|(\boldsymbol{\tau}, \mathbf{v})\|} + \frac{1}{\nu} \|\mathbf{u}_h\|_{\mathbf{M}} \|\mathbf{u} - \mathbf{u}_h\|_{\mathbf{M}}.
\end{aligned}$$

In this way, (5.5) follows straightforwardly from (3.12) and assumption (5.3). □

In turn, according to (3.4), (3.11) and the definition of the forms $\mathbf{a}$, $\mathbf{b}$ and $\mathbf{c}$, we find that, for any $(\boldsymbol{\tau}, \mathbf{v}) \in \mathbb{X}_0 \times \mathbf{M}$, there holds

$$\mathcal{R}(\boldsymbol{\tau}, \mathbf{v}) = \mathcal{R}_1(\boldsymbol{\tau}) + \mathcal{R}_2(\mathbf{v})$$

where

$$\mathcal{R}_1(\boldsymbol{\tau}) = \langle \boldsymbol{\tau}\mathbf{n}, \mathbf{u}_D \rangle_\Gamma - \frac{1}{\nu}(\boldsymbol{\sigma}_h^{\mathrm{d}}, \boldsymbol{\tau}^{\mathrm{d}})_\Omega - (\mathbf{u}_h, \mathbf{div}\, \boldsymbol{\tau})_\Omega - \frac{1}{\nu}\left(\mathbf{u}_h \otimes \mathbf{u}_h, \boldsymbol{\tau}^{\mathrm{d}}\right)_\Omega \tag{5.7}$$

and

$$\mathcal{R}_2(\mathbf{v}) = -(\mathbf{f}, \mathbf{v})_\Omega - (\mathbf{v}, \mathbf{div}\, \boldsymbol{\sigma}_h)_\Omega.$$

Hence, the supremum in (5.5) can be bounded in terms of $\mathcal{R}_1$ and $\mathcal{R}_2$ as follows

$$\|(\boldsymbol{\sigma} - \boldsymbol{\sigma}_h, \mathbf{u} - \mathbf{u}_h)\| \;\leq\; C_{glob} \left\{ \|\mathcal{R}_1\|_{\mathbb{X}_0'} + \|\mathcal{R}_2\|_{\mathbf{M}'} \right\}.$$

In this way, we have transformed (5.5) into an estimate involving global inf-sup conditions on $\mathbb{X}_0$ and $\mathbf{M}$, separately.

Throughout the rest of this section, we provide suitable upper bounds for $\mathcal{R}_1$ and $\mathcal{R}_2$. We begin by establishing the corresponding estimate for $\mathcal{R}_2$, whose proof follows from a straightforward application of the Hölder inequality.

Lemma 5.3 *There holds*

$$\|\mathcal{R}_2\|_{\mathbf{M}'} \leq \left\{ \sum_{T \in \mathcal{T}_h} \|\mathbf{f} + \mathbf{div}\, \boldsymbol{\sigma}_h\|_{\mathbf{L}^{4/3}(T)}^{4/3} \right\}^{3/4}.$$

Our next goal is to bound the remaining term $\|\mathcal{R}_1\|_{\mathbb{X}_0'}$. With this aim in mind, in what follows we introduce some technical results.

Lemma 5.4 *There exists $C_1 > 0$, independent of h, such that for each $\boldsymbol{\xi} \in \mathbb{W}^{1,4/3}(\Omega)$ there holds*

$$\left|\mathcal{R}_1(\boldsymbol{\xi} - \boldsymbol{\Pi}_h^k(\boldsymbol{\xi}))\right| \;\leq\; C_1 \left(\sum_{T \in \mathcal{T}_h} \Theta_{1,T}^2 \right)^{1/2} \|\boldsymbol{\xi}\|_{\mathbb{W}^{1,4/3}(\Omega)}, \tag{5.8}$$

where

$$\Theta_{1,T}^2 := h_T^{2-d/2} \left\| \nabla \mathbf{u}_h - \frac{1}{\nu}(\boldsymbol{\sigma}_h + (\mathbf{u}_h \otimes \mathbf{u}_h))^{\mathrm{d}} \right\|_{0,T}^2 + \sum_{e \in \mathcal{E}_{h,T}(\Gamma)} h_e^{1/2} \, \|\mathbf{u}_D - \mathbf{u}_h\|_{\mathbf{L}^4(e)}^2 \,.$$

Proof. We recall from the definition of $\mathcal{R}_1$ (cf. (5.7)) that

$$\begin{aligned} \mathcal{R}_1(\boldsymbol{\xi} - \boldsymbol{\Pi}_h^k(\boldsymbol{\xi})) \,&=\, \langle\, (\boldsymbol{\xi} - \boldsymbol{\Pi}_h^k(\boldsymbol{\xi}))\mathbf{n},\, \mathbf{u}_D \,\rangle_\Gamma - \frac{1}{\nu}\left(\boldsymbol{\sigma}_h^{\mathrm{d}},\, (\boldsymbol{\xi} - \boldsymbol{\Pi}_h^k(\boldsymbol{\xi}))^{\mathrm{d}}\right)_\Omega \\ &- \frac{1}{\nu}\left(\mathbf{u}_h,\, \mathbf{div}\,(\boldsymbol{\xi} - \boldsymbol{\Pi}_h^k(\boldsymbol{\xi}))\right)_\Omega - \frac{1}{\nu}\left(\mathbf{u}_h \otimes \mathbf{u}_h,\, (\boldsymbol{\xi} - \boldsymbol{\Pi}_h^k(\boldsymbol{\xi}))^{\mathrm{d}}\right). \end{aligned}$$

Applying a local integration by parts to the third term above, (4.1) and the fact that $\mathbf{u}_D \in \mathbf{L}^2(\Gamma)$, we obtain

$$\begin{aligned} \mathcal{R}_1(\boldsymbol{\xi} - \boldsymbol{\Pi}_h^k(\boldsymbol{\xi})) \;&=\; \sum_{e \in \mathcal{E}_h(\Gamma)} \Big((\boldsymbol{\xi} - \boldsymbol{\Pi}_h^k(\boldsymbol{\xi}))\mathbf{n},\, \mathbf{u}_D - \mathbf{u}_h \Big)_e \\ &+ \sum_{T \in \mathcal{T}_h} \left(\nabla \mathbf{u}_h - \frac{1}{\nu}(\boldsymbol{\sigma}_h + (\mathbf{u}_h \otimes \mathbf{u}_h))^{\mathrm{d}},\, (\boldsymbol{\xi} - \boldsymbol{\Pi}_h^k(\boldsymbol{\xi})) \right)_T . \end{aligned}$$

In turn, using Hölder and Cauchy-Schwarz inequalities, estimate (4.7) with $p = 4/3$, and the approximation property (see [39, eq. (3.28)] for details)

$$\|\tau \,-\, \Pi_h^k(\tau)\|_{0,T} \,\le\, C\, h_T^{1-d/4}\, |\tau|_{\mathbf{W}^{1,4/3}(T)} \quad \forall\, \tau \in \mathbf{W}^{1,4/3}(T)\,,$$

with $C > 0$ a constant independent of the meshsize, we obtain

$$\begin{aligned} \left|\mathcal{R}_1(\boldsymbol{\xi} - \boldsymbol{\Pi}_h^k(\boldsymbol{\xi}))\right| \;&\le\; \sum_{e \in \mathcal{E}_h(\Gamma)} \|\mathbf{u}_D - \mathbf{u}_h\|_{\mathbf{L}^4(e)}\, C\, h_e^{1/4}\, |\boldsymbol{\xi}|_{\mathbb{W}^{1,4/3}(T_e)} \\ &+ \sum_{T \in \mathcal{T}_h} \left\| \nabla \mathbf{u}_h - \frac{1}{\nu}(\boldsymbol{\sigma}_h + (\mathbf{u}_h \otimes \mathbf{u}_h))^{\mathrm{d}} \right\|_{0,T} C\, h_T^{1-d/4}\, |\boldsymbol{\xi}|_{\mathbb{W}^{1,4/3}(T)}, \end{aligned}$$

with T_e being the element that contains e.

Finally, from the subadditivity inequality we obtain

$$\begin{aligned} |\mathcal{R}_1(\boldsymbol{\xi} - \boldsymbol{\Pi}_h^k(\boldsymbol{\xi}))| \,\le\, \hat{C} \Bigg\{ & \left(\sum_{e \in \mathcal{E}_h(\Gamma)} h_e^{1/2}\, \|\mathbf{u}_D - \mathbf{u}_h\|_{\mathbf{L}^4(e)}^2 \right)^{1/2} \left(\sum_{e \in \mathcal{E}_h(\Gamma)} |\boldsymbol{\xi}|_{\mathbb{W}^{1,4/3}(T_e)}^{4/3} \right)^{3/4} \\ + & \left(\sum_{T \in \mathcal{T}_h} h_T^{2-d/2} \left\| \nabla \mathbf{u}_h - \frac{1}{\nu}(\boldsymbol{\sigma}_h + (\mathbf{u}_h \otimes \mathbf{u}_h))^{\mathrm{d}} \right\|_{0,T}^2 \right)^{1/2} \left(\sum_{T \in \mathcal{T}_h} |\boldsymbol{\xi}|_{\mathbb{W}^{1,4/3}(T)}^{4/3} \right)^{3/4} \Bigg\}, \end{aligned}$$

which clearly implies (5.8) and completes the proof. □

Lemma 5.5 *Assume that $\mathbf{u}_D \in \mathbf{H}^1(\Gamma)$ and let*

$$\begin{aligned} \Theta_{2,T}^2 \;&:=\; h_T^2 \left\| \underline{\mathbf{curl}} \left(\frac{1}{\nu}(\boldsymbol{\sigma}_h + (\mathbf{u}_h \otimes \mathbf{u}_h))^{\mathrm{d}} \right) \right\|_{0,T}^2 \\ &+ \sum_{e \in \mathcal{E}_{h,T}(\Omega)} h_e \left\| \left[\!\left[\boldsymbol{\gamma}_* \left(\frac{1}{\nu}(\boldsymbol{\sigma}_h + (\mathbf{u}_h \otimes \mathbf{u}_h))^{\mathrm{d}} \right) \right]\!\right] \right\|_{0,e}^2 \\ &+ \sum_{e \in \mathcal{E}_{h,T}(\Gamma)} h_e \left\| \boldsymbol{\gamma}_* \left(\frac{1}{\nu}(\boldsymbol{\sigma}_h + (\mathbf{u}_h \otimes \mathbf{u}_h))^{\mathrm{d}} - \nabla \mathbf{u}_D \right) \right\|_{0,e}^2 . \end{aligned}$$

Then,

a) if $d = 2$, there exists $C_2 > 0$, independent of h, such that

$$\left|\mathcal{R}_1\left(\mathbf{curl}\,(\mathbf{w} - \mathbf{I}_h\mathbf{w})\right)\right| \le C_2 \left(\sum_{T\in\mathcal{T}_h} \Theta_{2,T}^2\right)^{1/2} \|\mathbf{w}\|_{1,\Omega} \qquad \forall\, \mathbf{w} \in \mathbf{H}^1(\Omega). \tag{5.9}$$

b) if $d = 3$, there exists $\hat{C}_2 > 0$, independent of h, such that

$$\left|\mathcal{R}_1\left(\underline{\mathbf{curl}}\,(\mathbf{w} - \mathbf{I}_h\mathbf{w})\right)\right| \le \hat{C}_2 \left(\sum_{T\in\mathcal{T}_h} \Theta_{2,T}^2\right)^{1/2} \|\mathbf{w}\|_{1,\Omega} \qquad \forall\, \mathbf{w} \in \mathbb{H}^1(\Omega).$$

Proof. In what follows we prove the result for $d = 2$ since the three dimensional follows analogously.

Given $\mathbf{w} \in \mathbf{H}^1(\Omega)$, we first notice from the definition of $\mathcal{R}_1$ in (5.7) that there holds

$$\mathcal{R}_1(\mathbf{curl}\,(\mathbf{w} - \mathbf{I}_h\mathbf{w})) = \langle \mathbf{curl}\,(\mathbf{w} - \mathbf{I}_h\mathbf{w})\mathbf{n}, \mathbf{u}_D\rangle_\Gamma - \frac{1}{\nu}\left(\boldsymbol{\sigma}_h^{\mathrm{d}} + (\mathbf{u}_h \otimes \mathbf{u}_h)^{\mathrm{d}}, \mathbf{curl}\,(\mathbf{w} - \mathbf{I}_h\mathbf{w})\right)_\Omega.$$

Recalling that $\mathbf{u}_D \in \mathbf{H}^1(\Gamma)$, now we apply the following integration by parts on the boundary Γ given by (see, for instance, [21, Lemma 3.5, eq. (3.34)])

$$\langle \mathbf{curl}\,(\mathbf{w} - \mathbf{I}_h\mathbf{w})\mathbf{n}, \mathbf{u}_D\rangle_\Gamma = \langle \nabla\mathbf{u}_D\boldsymbol{s}, \mathbf{w} - \mathbf{I}_h\mathbf{w}\rangle_\Gamma = \langle \boldsymbol{\gamma}_*(\nabla\mathbf{u}_D), \mathbf{w} - \mathbf{I}_h\mathbf{w}\rangle_\Gamma,$$

and a local integration by parts, to obtain

$$\begin{aligned}
\mathcal{R}_1(\mathbf{curl}\,(\mathbf{w} - \mathbf{I}_h\mathbf{w})) \;&=\; -\sum_{T\in\mathcal{T}_h}\left(\underline{\mathbf{curl}}\left(\frac{1}{\nu}(\boldsymbol{\sigma}_h + (\mathbf{u}_h \otimes \mathbf{u}_h))^{\mathrm{d}}\right), \mathbf{w} - \mathbf{I}_h\mathbf{w}\right)_T \\
&+ \sum_{e\in\mathcal{E}_h(\Omega)}\left(\left[\!\left[\boldsymbol{\gamma}_*\left(\frac{1}{\nu}(\boldsymbol{\sigma}_h + (\mathbf{u}_h \otimes \mathbf{u}_h))^{\mathrm{d}}\right)\right]\!\right], \mathbf{w} - \mathbf{I}_h\mathbf{w}\right)_e \\
&+ \sum_{e\in\mathcal{E}_h(\Gamma)}\left(\boldsymbol{\gamma}_*\left(\frac{1}{\nu}(\boldsymbol{\sigma}_h + (\mathbf{u}_h \otimes \mathbf{u}_h))^{\mathrm{d}} - \nabla\mathbf{u}_D\right), \mathbf{w} - \mathbf{I}_h\mathbf{w}\right)_e.
\end{aligned}$$

Hence, applying Cauchy-Schwarz inequality and the approximation properties of the Clément interpolant (cf. Lemma 4.3), we obtain

$$\begin{aligned}
&\left|\mathcal{R}_1(\mathbf{curl}\,(\mathbf{w} - \mathbf{I}_h\mathbf{w}))\right| \\
&\le \hat{C}\left\{\left(\sum_{T\in\mathcal{T}_h} h_T^2 \left\|\underline{\mathbf{curl}}\left(\frac{1}{\nu}(\boldsymbol{\sigma}_h + (\mathbf{u}_h \otimes \mathbf{u}_h))^{\mathrm{d}}\right)\right\|_{0,T}^2\right)^{1/2}\left(\sum_{T\in\mathcal{T}_h}\|\mathbf{w}\|_{1,\Delta(T)}^2\right)^{1/2}\right. \\
&+ \left(\sum_{e\in\mathcal{E}_h(\Omega)} h_e \left\|\left[\!\left[\boldsymbol{\gamma}_*\left(\frac{1}{\nu}(\boldsymbol{\sigma}_h + (\mathbf{u}_h \otimes \mathbf{u}_h))^{\mathrm{d}}\right)\right]\!\right]\right\|_{0,e}^2\right)^{1/2}\left(\sum_{e\in\mathcal{E}_h(\Omega)}\|\mathbf{w}\|_{1,\Delta(e)}^2\right)^{1/2} \\
&+ \left.\left(\sum_{e\in\mathcal{E}_h(\Gamma)} h_e \left\|\boldsymbol{\gamma}_*\left(\frac{1}{\nu}(\boldsymbol{\sigma}_h + (\mathbf{u}_h \otimes \mathbf{u}_h))^{\mathrm{d}} - \nabla\mathbf{u}_D\right)\right\|_{0,e}^2\right)^{1/2}\left(\sum_{e\in\mathcal{E}_h(\Gamma)}\|\mathbf{w}\|_{1,\Delta(e)}^2\right)^{1/2}\right\}.
\end{aligned}$$

Therefore, from the previous estimate and the fact that the number of triangles of the macro-elements $\Delta(T)$ and $\Delta(e)$ are uniformly bounded, we get (5.9) and conclude the proof. $\square$

The following lemma combines Lemmas 5.4 and 5.5 and establishes the desired estimate for $\mathcal{R}_1$.

Lemma 5.6 *There exists $C > 0$, independent of h, such that*

$$\|\mathcal{R}_1\|_{\mathbb{X}_0'} \leq C \left\{ \sum_{T\in\mathcal{T}_h} \Theta_T^2 \right\}^{1/2},$$

with Θ_T defined as in (5.2).

Proof. For simplicity, we prove the result for the two-dimensional case. The three dimensional case proceed analogously.

Let $\boldsymbol{\tau} \in \mathbb{X}_0$. It follows from Lemma 4.4 that there exist $\boldsymbol{\xi} \in \mathbb{W}^{1,4/3}(\Omega)$ and $\mathbf{w} \in \mathbf{H}^1(\Omega)$, such that $\boldsymbol{\tau} = \boldsymbol{\xi} + \mathbf{curl}\,\mathbf{w}$ and

$$\|\boldsymbol{\xi}\|_{\mathbb{W}^{1,4/3}(\Omega)} + \|\mathbf{w}\|_{1,\Omega} \leq C_{Hel}\|\boldsymbol{\tau}\|_{\mathbb{X}}. \tag{5.10}$$

Now, noticing that owing to the Galerkin orthogonality there holds $\mathcal{R}_1(\boldsymbol{\tau}_h) = 0$ for all $\boldsymbol{\tau}_h \in \mathbb{X}_{h,0}$, it follows that

$$\mathcal{R}_1(\boldsymbol{\tau}) = \mathcal{R}_1(\boldsymbol{\tau} - \boldsymbol{\tau}_h) \quad \forall \boldsymbol{\tau}_h \in \mathbb{X}_{h,0}.$$

In particular, for $\boldsymbol{\tau}_h$ defined as

$$\boldsymbol{\tau}_h = \boldsymbol{\Pi}_h^k\boldsymbol{\xi} + \mathbf{curl}\,(\mathbf{I}_h\mathbf{w}) + C_{\boldsymbol{\xi},\mathbf{w}}\mathbb{I}, \text{ with } C_{\boldsymbol{\xi},\mathbf{w}} = -\frac{1}{2|\Omega|}\Big(\mathrm{tr}\left(\boldsymbol{\Pi}_h^k(\boldsymbol{\xi}) + \mathbf{curl}\,(\mathbf{I}_h\mathbf{w})\right), 1\Big)_{\Omega},$$

and observing that from the definition of $\mathcal{R}_1$ and the compatibility condition (3.2), there holds $\mathcal{R}_1(c\,\mathbb{I}) = 0$ for any constant $c \in \mathbb{R}$, we obtain

$$\mathcal{R}_1(\boldsymbol{\tau}) = \mathcal{R}_1(\boldsymbol{\xi} - \boldsymbol{\Pi}_h^k\xi) + \mathcal{R}_1(\mathbf{curl}\,(\mathbf{w} - \mathbf{I}_h\mathbf{w})).$$

Hence, the proof follows from Lemmas 5.4 and 5.5, and estimate (5.10). $\square$

We end this section by observing that the reliability estimate (5.4) is a direct consequence of Lemmas 5.3 and 5.6.

5.2 Local efficiency of the a posteriori error estimator

We begin by establishing the main result of this section.

Theorem 5.7 *There exists $C_{rel} > 0$, independent of h, such that*

$$C_{eff}\,\Theta \leq \|(\boldsymbol{\sigma} - \boldsymbol{\sigma}_h, \mathbf{u} - \mathbf{u}_h)\| + \text{h.o.t}, \tag{5.11}$$

where h.o.t. *stands for one or several terms of higher order.*

We remark in advance that the proof of (5.11) makes frequent use of the identities provided by Theorem 3.2. We begin with the estimates for the zero order terms appearing in the definition of Θ_T (cf. (5.2)).

Lemma 5.8 *There holds*

$$\|\mathbf{f} + \mathbf{div}\,\boldsymbol{\sigma}_h\|_{\mathbf{L}^{4/3}(T)} \le \|\boldsymbol{\sigma} - \boldsymbol{\sigma}_h\|_{\mathbf{div}_{4/3},T} \quad \forall\, T \in \mathcal{T}_h.$$

Proof. It suffices to recall, as established in Theorem 3.2, that $\mathbf{f} = -\mathbf{div}\,\boldsymbol{\sigma}$ in Ω. □

In order to derive the upper bounds for the remaining terms defining the global *a posteriori* error estimator Θ (cf.(5.1)), we use results from [13], inverse inequalities, and the localization technique based on element-bubble and edge-bubble functions. To this end, we now introduce further notations and preliminary results. Given $T \in \mathcal{T}_h$ and $e \in \mathcal{E}_{h,T}$, we let ϕ_T and ϕ_e be the usual element-bubble and edge(face)-bubble functions, respectively (see [43] for details). In particular ϕ_T satisfies $\phi_T \in P_3(T)$, $supp\,\phi_T \subseteq T$, $\phi_T = 0$ on ∂T, and $0 \le \phi_T \le 1$ in T. Similarly, $\phi_e|_T \in P_2(T)$, $supp\,\phi_e \subseteq \omega_e := \cup\{T' \in \mathcal{T}_h : e \in \mathcal{E}_{h,T'}\}$, $\phi_e = 0$ on $\partial T \backslash e$ and $0 \le \phi_T \le 1$ in ω_e. We also recall from [43] that, given $k \in \mathbb{N} \cup \{0\}$, there exists an extension operator $L : C(e) \to C(\omega_e)$ that satisfies $L(p) \in P_k(T)$ and $L(p)|_e = p\ \forall\, p \in P_k(e)$. A corresponding vector version of L, that is the componentwise application of L, is denoted by $\mathbf{L}$. Additional properties of ϕ_T, ϕ_e and L are collected in the following lemma.

Lemma 5.9 *Given $k \in \mathbb{N} \cup \{0\}$, there exist positive constants c_1, c_2, c_3 and c_4, depending only on k and the shape regularity of the triangulations (minimum angle condition), such that, for each triangle T and $e \in \mathcal{E}_h$, there hold*

$$\|\phi_T q\|_{0,T}^2 \le \|q\|_{0,T}^2 \le c_1 \|\phi_T^{1/2} q\|_{0,T}^2 \quad \forall q \in P_k(T), \tag{5.12}$$

$$\|\phi_e L(p)\|_{0,e}^2 \le \|p\|_{0,e}^2 \le c_2 \|\phi_e^{1/2} p\|_{0,e}^2 \quad \forall p \in P_k(e)$$

and

$$c_3\, h_e^{1/2} \|p\|_{0,e} \le \|\phi_e^{1/2} L(p)\|_{0,T} \le c_4\, h_e^{1/2} \|p\|_{0,e} \quad \forall p \in P_k(e).$$

Proof. See Lemma 4.1 in [43]. □

In addition, given $k \in \mathbb{N} \cup \{0\}$, $T \in \mathcal{T}_h$ and $e \in \mathcal{E}_h$, in what follows we will make use of the following inverse inequalities (see [22, Lemma 1.138]): There exist c_1, $c_2 > 0$, independent of the meshsize, such that

$$\|v\|_{\mathrm{W}^{1,4/3}(T)} \le c_1\, h_T^{-1+d/4} \|v\|_{0,T} \qquad \forall\, v \in P_k(T), \tag{5.13}$$

$$\|v\|_{\mathrm{L}^4(e)} \le c_2\, h_e^{(1-d)/4} \|v\|_{0,e} \qquad \forall\, v \in P_k(e). \tag{5.14}$$

Now we recall the well-known inverse inequality result.

Finally, we recall the standard discrete trace inequality, which establishes the existence of a positive constant c, depending only on the shape regularity of the triangulations, such that for each $T \in \mathcal{T}_h$ and $e \in \mathcal{E}_{h,T}$, there holds

$$\|v\|_{0,e}^2 \le c \left(h_e^{-1} \|v\|_{0,T}^2 + h_e |v|_{1,T}^2 \right) \quad \forall\, v \in H^1(T). \tag{5.15}$$

The proof of (5.15) we refer to Theorem 3.10 in [1].

Now we proceed by deriving the estimates for the remaining terms defining Θ.

Lemma 5.10 *There exists $C_1 > 0$, independent of h, such that*

$$\begin{aligned} h_T^{1-d/4} \left\| \nabla \mathbf{u}_h - \frac{1}{\nu}(\boldsymbol{\sigma}_h + (\mathbf{u}_h \otimes \mathbf{u}_h))^{\mathrm{d}} \right\|_{0,T} \\ \leq C_1 \Big\{ \big(1 + h_T^{1-d/4}\big) \|\mathbf{u} - \mathbf{u}_h\|_{\mathbf{L}^4(T)} + h_T^{1-d/4} \big\|\boldsymbol{\sigma} - \boldsymbol{\sigma}_h\big\|_{0,T} \Big\} \quad \forall\, T \in \mathcal{T}_h. \end{aligned} \tag{5.16}$$

Proof. Given $T \in \mathcal{T}_h$, we define $\boldsymbol{\chi}_T := \nabla \mathbf{u}_h - \dfrac{1}{\nu}(\boldsymbol{\sigma}_h + (\mathbf{u}_h \otimes \mathbf{u}_h))^{\mathrm{d}}$ in T. Then, applying (5.12) to $\|\boldsymbol{\chi}_T\|_{0,T}$, recalling the identity $\nabla \mathbf{u} = \dfrac{1}{\nu}(\boldsymbol{\sigma} + (\mathbf{u} \otimes \mathbf{u}))^{\mathrm{d}}$ in Ω (cf. Theorem 3.2), integrating by parts and using that $\phi_T = 0$ on ∂T, we deduce

$$\begin{aligned} \|\boldsymbol{\chi}_T\|_{0,T}^2 \leq \|\phi_T^{1/2} \boldsymbol{\chi}_T\|_{0,T}^2 = \left(\nabla \mathbf{u}_h - \frac{1}{\nu}(\boldsymbol{\sigma}_h + (\mathbf{u}_h \otimes \mathbf{u}_h))^{\mathrm{d}}, \phi_T \boldsymbol{\chi}_T \right)_T \\ = (\mathbf{div}\,(\phi_T \boldsymbol{\chi}_T), \mathbf{u} - \mathbf{u}_h)_T + \frac{1}{\nu} \left(\phi_T \boldsymbol{\chi}_T, (\boldsymbol{\sigma}^{\mathrm{d}} - \boldsymbol{\sigma}_h^{\mathrm{d}}) + (\mathbf{u} \otimes \mathbf{u})^{\mathrm{d}} - (\mathbf{u}_h \otimes \mathbf{u}_h)^{\mathrm{d}} \right)_T . \end{aligned}$$

Next, using the Hölder and Cauchy-Schwarz inequalities, the inverse inequality (5.13) with $l = 1$, $p = 4/3$, $m = 0$ and $q = 2$, and the estimate (5.12), we obtain

$$\begin{aligned} \|\boldsymbol{\chi}_T\|_{0,T}^2 \leq c |\phi_T \boldsymbol{\chi}_T|_{\mathbf{W}^{1,4/3}(T)} \|\mathbf{u} - \mathbf{u}_h\|_{\mathbf{L}^4(T)} + \frac{1}{\nu} \|\phi_T \boldsymbol{\chi}_T\|_{0,T} \left\| (\boldsymbol{\sigma} - \boldsymbol{\sigma}_h)^{\mathrm{d}} + (\mathbf{u} \otimes \mathbf{u} - \mathbf{u}_h \otimes \mathbf{u}_h)^{\mathrm{d}} \right\|_{0,T} \\ \leq C\, h_T^{-1+d/4} \|\boldsymbol{\chi}_T\|_{0,T} \|\mathbf{u} - \mathbf{u}_h\|_{\mathbf{L}^4(T)} + \frac{1}{\nu} \|\boldsymbol{\chi}_T\|_{0,T} \left(\big\|\boldsymbol{\sigma} - \boldsymbol{\sigma}_h\big\|_{0,T} + \big\|\mathbf{u} \otimes \mathbf{u} - \mathbf{u}_h \otimes \mathbf{u}_h\big\|_{0,T} \right), \end{aligned}$$

which implies

$$\|\boldsymbol{\chi}_T\|_{0,T} \leq C\, h_T^{-1+d/4} \|\mathbf{u} - \mathbf{u}_h\|_{\mathbf{L}^4(T)} + \frac{1}{\nu} \left(\big\|\boldsymbol{\sigma} - \boldsymbol{\sigma}_h\big\|_{0,T} + \big\|\mathbf{u} \otimes \mathbf{u} - \mathbf{u}_h \otimes \mathbf{u}_h\big\|_{0,T} \right). \tag{5.17}$$

In turn, applying similar algebraic manipulation used in [10, Corollary 4.10], using Hölder inequality, estimates (3.10), (3.12), and the fact that the data are small enough, we deduce that

$$\big\|\mathbf{u} \otimes \mathbf{u} - \mathbf{u}_h \otimes \mathbf{u}_h\big\|_{0,T} \leq \left(\|\mathbf{u}\|_{\mathbf{L}^4(T)} + \|\mathbf{u}_h\|_{\mathbf{L}^4(T)} \right) \|\mathbf{u} - \mathbf{u}_h\|_{\mathbf{L}^4(T)} \leq C\, \|\mathbf{u} - \mathbf{u}_h\|_{\mathbf{L}^4(T)}, \tag{5.18}$$

with $C > 0$ independent of h. Finally, replacing (5.18) into (5.17) we obtain (5.16) and conclude the proof. □

Lemma 5.11 *Assume that $\mathbf{u}_D$ is piecewise polynomial. Then, there exists $C_2 > 0$, independent of h, such that*

$$h_e^{1/4} \|\mathbf{u}_D - \mathbf{u}_h\|_{\mathbf{L}^4(e)} \leq C_2 \Big\{ \big(1 + h_T^{1-d/4}\big) \|\mathbf{u} - \mathbf{u}_h\|_{\mathbf{L}^4(T)} + h_T^{1-d/4} \big\|\boldsymbol{\sigma} - \boldsymbol{\sigma}_h\big\|_{0,T} \Big\} \tag{5.19}$$

for all $e \in \mathcal{E}_{h,T}(\Gamma)$.

Proof. Given $e \in \mathcal{E}_h(\Gamma)$, from (5.14), it follows that

$$\|\mathbf{u}_D - \mathbf{u}_h\|_{\mathbf{L}^4(e)} \leq C h_e^{(1-d)/4} \|\mathbf{u}_D - \mathbf{u}_h\|_{0,e}. \tag{5.20}$$

Hence, from (5.20) and (5.15), we deduce that

$$\|\mathbf{u}_D - \mathbf{u}_h\|_{\mathbf{L}^4(e)} \leq C \left\{ h_e^{(-1-d)/4} \|\mathbf{u} - \mathbf{u}_h\|_{0,T} + h_e^{(3-d)/4} |\mathbf{u} - \mathbf{u}_h|_{1,T} \right\}. \tag{5.21}$$

Now, using the Cauchy-Schwarz inequality and the fact that $|T| \cong h_T^d$, we deduce that

$$\|\mathbf{u} - \mathbf{u}_h\|_{0,T} = \big(1, |\mathbf{u} - \mathbf{u}_h|^2\big)_T^{1/2} \leq |T|^{1/4} \|\mathbf{u} - \mathbf{u}_h\|_{\mathbf{L}^4(T)} \leq c h_T^{d/4} \|\mathbf{u} - \mathbf{u}_h\|_{\mathbf{L}^4(T)}. \tag{5.22}$$

In turn, using the identity $\nabla \mathbf{u} = \dfrac{1}{\nu}(\boldsymbol{\sigma}^{\mathrm{d}} + (\mathbf{u} \otimes \mathbf{u})^{\mathrm{d}})$ in Ω (cf. Theorem 3.2) and some algebraic computations, we deduce that

$$\begin{aligned} |\mathbf{u} - \mathbf{u}_h|_{1,T} &= \left\| \frac{1}{\nu} \Big((\boldsymbol{\sigma} - \boldsymbol{\sigma}_h)^{\mathrm{d}} + ((\mathbf{u} \otimes \mathbf{u}) - (\mathbf{u}_h \otimes \mathbf{u}_h))^{\mathrm{d}} \Big) + \frac{1}{\nu} \left(\boldsymbol{\sigma}_h + (\mathbf{u}_h \otimes \mathbf{u}_h) \right)^{\mathrm{d}} - \nabla \mathbf{u}_h \right\|_{0,T} \\ &\leq \frac{1}{\nu} \left(\|\boldsymbol{\sigma} - \boldsymbol{\sigma}_h\|_{0,T} + \big\|\mathbf{u} \otimes \mathbf{u} - \mathbf{u}_h \otimes \mathbf{u}_h\big\|_{0,T} \right) + \left\| \nabla \mathbf{u}_h - \frac{1}{\nu} \left(\boldsymbol{\sigma}_h + (\mathbf{u}_h \otimes \mathbf{u}_h) \right)^{\mathrm{d}} \right\|_{0,T} \end{aligned}$$

which together with (5.17) and (5.18), yields

$$|\mathbf{u} - \mathbf{u}_h|_{1,T} \leq C \left(1 + h_T^{-1+d/4}\right) \|\mathbf{u} - \mathbf{u}_h\|_{\mathbf{L}^4(T)} + \frac{2}{\nu} \|\boldsymbol{\sigma} - \boldsymbol{\sigma}_h\|_{0,T}. \tag{5.23}$$

Therefore, (5.19) follows from estimates (5.21), (5.22) and (5.23), and the fact that $h_e \leq h_T$. □

Now we establish the estimates for the remaining terms defining Θ.

Lemma 5.12 *There exist $C_3 > 0$ and $C_4 > 0$, independent of h, such that*

$$h_T \left\| \underline{\mathbf{curl}} \left(\frac{1}{\nu} (\boldsymbol{\sigma}_h + (\mathbf{u}_h \otimes \mathbf{u}_h))^{\mathrm{d}} \right) \right\|_{0,T} \leq C_3 \Big\{ \|\mathbf{u} - \mathbf{u}_h\|_{\mathbf{L}^4(T)} + \|\boldsymbol{\sigma} - \boldsymbol{\sigma}_h\|_{0,T} \Big\} \tag{5.24}$$

for all $T \in \mathcal{T}_h$ and

$$h_e^{1/2} \left\| \left[\!\left[\boldsymbol{\gamma}_* \left(\frac{1}{\nu} (\boldsymbol{\sigma}_h + (\mathbf{u}_h \otimes \mathbf{u}_h))^{\mathrm{d}} \right) \right]\!\right] \right\|_{0,e} \leq C_4 \Big\{ \|\mathbf{u} - \mathbf{u}_h\|_{\mathbf{L}^4(\omega_e)} + \|\boldsymbol{\sigma} - \boldsymbol{\sigma}_h\|_{0,\omega_e} \Big\} \tag{5.25}$$

for all $e \in \mathcal{E}_h(\Omega)$.

Additionally, if $\mathbf{u}_D$ is piecewise polynomial, there exists $C_5 > 0$, independent of h, such that

$$h_e^{1/2} \left\| \boldsymbol{\gamma}_* \left(\frac{1}{\nu} (\boldsymbol{\sigma}_h + (\mathbf{u}_h \otimes \mathbf{u}_h))^{\mathrm{d}} - \nabla \mathbf{u}_D \right) \right\|_{0,e} \leq C_5 \Big\{ \|\mathbf{u} - \mathbf{u}_h\|_{\mathbf{L}^4(T_e)} + \|\boldsymbol{\sigma} - \boldsymbol{\sigma}_h\|_{0,T_e} \Big\} \tag{5.26}$$

for all $e \in \mathcal{E}_h(\Gamma)$, where T_e is the element to which the boundary edge or boundary face e belongs.

Proof. For the two-dimensional case, we proceed as in [20, Lemma 3.15], that is, we apply [28, Lemmas 4.9, 4.10, and 4.15] to $\boldsymbol{\zeta} := \dfrac{1}{\nu}(\boldsymbol{\sigma} + (\mathbf{u} \otimes \mathbf{u}))^{\mathrm{d}} = \nabla \mathbf{u}$ and $\boldsymbol{\zeta}_h := \dfrac{1}{\nu}(\boldsymbol{\sigma}_h + (\mathbf{u}_h \otimes \mathbf{u}_h))^{\mathrm{d}}$, and the estimate $\|(\mathbf{u} \otimes \mathbf{u})^{\mathrm{d}} - (\mathbf{u}_h \otimes \mathbf{u}_h)^{\mathrm{d}}\|_{0,T} \leq \|\mathbf{u} \otimes \mathbf{u} - \mathbf{u}_h \otimes \mathbf{u}_h\|_{0,T}$, to obtain

$$\left\| \underline{\mathbf{curl}} \left(\frac{1}{\nu} (\boldsymbol{\sigma}_h + \mathbf{u}_h \otimes \mathbf{u}_h)^{\mathrm{d}} \right) \right\|_{0,T}^2 \leq C h_T^{-2} \Big\{ \|\boldsymbol{\sigma} - \boldsymbol{\sigma}_h\|_{0,T}^2 + \|\mathbf{u} \otimes \mathbf{u} - \mathbf{u}_h \otimes \mathbf{u}_h\|_{0,T}^2 \Big\}, \tag{5.27}$$

$$\left\| \left[\!\left[\boldsymbol{\gamma}_* \left(\frac{1}{\nu} (\boldsymbol{\sigma}_h + \mathbf{u}_h \otimes \mathbf{u}_h)^{\mathrm{d}} \right) \right]\!\right] \right\|_{0,e}^2 \leq C h_e^{-1} \Big\{ \|\boldsymbol{\sigma} - \boldsymbol{\sigma}_h\|_{0,\omega_e}^2 + \|\mathbf{u} \otimes \mathbf{u} - \mathbf{u}_h \otimes \mathbf{u}_h\|_{0,\omega_e}^2 \Big\} \tag{5.28}$$

and

$$\left\|\gamma_*\left(\frac{1}{\nu}(\boldsymbol{\sigma}_h + \mathbf{u}_h \otimes \mathbf{u}_h)^{\mathrm{d}} - \nabla \mathbf{u}_D\right)\right\|_{0,e}^2 \le C h_e^{-1} \Big\{ \|\boldsymbol{\sigma} - \boldsymbol{\sigma}_h\|_{0,T_e}^2 + \|\mathbf{u} \otimes \mathbf{u} - \mathbf{u}_h \otimes \mathbf{u}_h\|_{0,T_e}^2 \Big\}. \quad (5.29)$$

Thus, using the estimate (5.18) it follows that (5.27), (5.28), and (5.29), imply (5.24), (5.25), and (5.26), respectively. On the other hand, for the three-dimensional case the corresponding estimates follow from using the results from Lemmas 4.9, 4.10, and 4.13 in [26], respectively. □

We remark that, for simplicity, we have assume that $\mathbf{u}_D$ to be piecewise polynomial for the derivation of (5.19) in Lemma 5.11 and (5.26) in Lemma 5.12. However, by assuming that $\mathbf{u}_D$ is sufficiently smooth, and proceeding similarly as in [15, Section 6.2] one can also obtain similar estimates. In such a case, higher order terms given by the errors arising from suitable polynomial approximations would appear in (5.19) and (5.26), which explains the eventual h.o.t in (5.11).

We end this section by remarking that the efficiency of Θ (cf. (5.11)) in Theorem 5.7 is now a straightforward consequence of Lemmas 5.8, 5.10, 5.11 and 5.12. In turn, we emphasize that the resulting positive constant, denoted by C_{eff} is independent of h.

6 Numerical results

This section serves to illustrate the performance and accuracy of our mixed finite element scheme (3.11) along with the reliability and efficiency properties of the *a posteriori* error estimator Θ (cf. (5.1)) derived in Section 5. In what follows, we refer to the corresponding sets of finite element subspaces generated by $k = 0$ and $k = 1$, as simply $\mathbb{RT}_0 - \mathbf{P}_0$ and $\mathbb{RT}_1 - \mathbf{P}_1$, respectively. Our implementation is based on a FreeFem++ code [32]. Regarding the implementation of the Newton iterative method associated to (3.11) (see [10, Section 5] for details), the iterations are terminated once the relative error of the entire coefficient vectors between two consecutive iterates is sufficiently small, i.e.,

$$\frac{\|\mathsf{coeff}^{m+1} - \mathsf{coeff}^m\|_{\ell^2}}{\|\mathsf{coeff}^{m+1}\|_{\ell^2}} \le \mathsf{tol},$$

where $\|\cdot\|_{\ell^2}$ is the standard ℓ^2-norm in $\mathbb{R}^N$, with N denoting the total number of degrees of freedom defining the finite element subspaces $\mathbb{X}_h$ and $\mathbf{M}_h$ stated in Section 3.3, and tol is a fixed tolerance chosen as tol=1E-06. As usual, the individual errors are denoted by:

$$\mathsf{e}(\boldsymbol{\sigma}) := \|\boldsymbol{\sigma} - \boldsymbol{\sigma}_h\|_{\mathbb{X}}, \quad \mathsf{e}(\mathbf{u}) := \|\mathbf{u} - \mathbf{u}_h\|_{\mathbf{M}}, \quad \mathsf{e}(p) := \|p - p_h\|_{0,\Omega},$$
$$\mathsf{e}(\nabla \mathbf{u}) := \|\nabla \mathbf{u} - \mathbf{G}_h\|_{0,\Omega}, \quad \mathsf{e}(\boldsymbol{\omega}) := \|\boldsymbol{\omega} - \boldsymbol{\omega}_h\|_{0,\Omega},$$

where the pressure p, the velocity gradient $\nabla \mathbf{u}$, and the vorticity $\boldsymbol{\omega} := \frac{1}{2}\left(\nabla \mathbf{u} - (\nabla \mathbf{u})^{\mathrm{t}}\right)$ are approximated, respectively, through the post-processing formulas (cf. [10, Section 4.4]):

$$p_h = -\frac{1}{d}\left(\operatorname{tr}(\boldsymbol{\sigma}_h) + \operatorname{tr}(\mathbf{u}_h \otimes \mathbf{u}_h) - \frac{1}{|\Omega|}(\operatorname{tr}(\mathbf{u}_h \otimes \mathbf{u}_h), 1)_\Omega\right),$$
$$\mathbf{G}_h = \frac{1}{\nu}\left(\boldsymbol{\sigma}_h^{\mathrm{d}} + (\mathbf{u}_h \otimes \mathbf{u}_h)^{\mathrm{d}}\right), \quad \boldsymbol{\omega}_h = \frac{1}{2\nu}\left(\boldsymbol{\sigma}_h - \boldsymbol{\sigma}_h^{\mathrm{t}}\right).$$

Then, the global error and the effectivity index associated to the global estimator Θ are denoted, respectively, by

$$\mathsf{e}(\boldsymbol{\sigma},\mathbf{u}) := \mathsf{e}(\boldsymbol{\sigma}) + \mathsf{e}(\mathbf{u}) \quad \text{and} \quad \mathsf{eff}(\Theta) := \frac{\mathsf{e}(\boldsymbol{\sigma},\mathbf{u})}{\Theta}.$$

Moreover, using the fact that $c\,N^{-1/d} \le h \le C\,N^{-1/d}$, the experimental rate of convergence of any of the above quantities will be computed as

$$\mathsf{r}(\diamond) := -d\,\frac{\log(\mathsf{e}(\diamond)/\mathsf{e}'(\diamond))}{\log(N/N')} \quad \text{for each } \diamond \in \Big\{\boldsymbol{\sigma},\mathbf{u},p,\nabla\mathbf{u},\boldsymbol{\omega},(\boldsymbol{\sigma},\mathbf{u})\Big\},$$

where N and N' denote the total degrees of freedom associated to two consecutive triangulations with errors e and e'.

The examples to be considered in this section are described next. In all of them, for the sake of simplicity, we choose the parameter $\nu = 1$. Furthermore, the condition $(\mathrm{tr}(\boldsymbol{\sigma}_h),1)_\Omega = 0$ is imposed via a penalization strategy using a scalar Lagrange multiplier (see [10, eq. (5.1)] for details).

Example 1 is used to corroborate the reliability and efficiency of the *a posteriori* error estimator Θ, whereas Examples 2 and 3 are utilized to illustrate the behavior of the associated adaptive algorithm in 2D and 3D domains, respectively, which applies the following procedure from [44]:

(1) Start with a coarse mesh $\mathcal{T}_h$.

(2) Solve the Newton iterative method associated to (3.11) for the current mesh $\mathcal{T}_h$.

(3) Compute the local indicator $\widehat{\Theta}_T$ for each $T \in \mathcal{T}_h$, where

$$\widehat{\Theta}_T := \Theta_T + \|\mathbf{f} + \mathbf{div}\,\boldsymbol{\sigma}_h\|_{\mathbf{L}^{4/3}(T)}, \qquad \text{(cf. (5.2))}$$

(4) Check the stopping criterion and decide whether to finish or go to next step.

(5) Generate an adapted mesh through a variable metric/Delaunay automatic meshing algorithm (see [33, Section 9.1.9]).

(6) Define resulting mesh as current mesh $\mathcal{T}_h$, and go to step (2).

Example 1: Accuracy assessment with a smooth solution in a square domain.

In our first example, we concentrate on the accuracy of the mixed method. We consider the square domain $\Omega := (0,1)^2$. The data $\mathbf{f}$ and $\mathbf{u}_D$ are chosen so that a manufactured solution of (3.1) is given by the smooth functions

$$\mathbf{u}(\mathbf{x}) := \begin{pmatrix} x_1^2(x_1-1)^2\sin(x_2) \\ 2x_1(x_1-1)(2x_1-1)\cos(x_2) \end{pmatrix},$$

$$p(\mathbf{x}) := \cos(\pi x_1)\exp(\pi x_2) \quad \forall\,\mathbf{x} := (x_1,x_2) \in \Omega.$$

The results reported in Tables 6.1 and 6.2 are in accordance with the theoretical bounds established in Theorem 3.4. In addition, we also compute the global *a posteriori* error indicator Θ (cf. (5.1)), and measure its reliability and efficiency with the effectivity index. Notice that the estimator remain always bounded.

Example 2: Adaptivity in a 2D L-shape domain.

Our second example is aimed at testing the features of adaptive mesh refinement after the *a posteriori* error estimator Θ (cf. (5.1)). We consider a L-shape contraction domain $\Omega := (-1,1)^2 \setminus (0,1)^2$. The data $\mathbf{f}$ and $\mathbf{u}_D$ are chosen so that the exact solution is given by

$$\mathbf{u}(\mathbf{x}) := \begin{pmatrix} -\cos(\pi x_1)\sin(\pi x_2) \\ \sin(\pi x_1)\cos(\pi x_2) \end{pmatrix},$$

$$p(\mathbf{x}) := \frac{1 - x_1}{(x_1 - 0.02)^2 + (x_2 - 0.02)^2} - p_0 \quad \forall\, \mathbf{x} := (x_1, x_2) \in \Omega,$$

where $p_0 \in \mathbb{R}$ is a constant chosen in such a way $(p,1)_\Omega = 0$. Notice that the pressure exhibit high gradients near the vertex $(0,0)$.

Tables 6.3–6.6 along with Figure 6.1, summarizes the convergence history of the method applied to a sequence of quasi-uniformly and adaptively refined triangulation of the domain. Suboptimal rates are observed in the first case, whereas adaptive refinement according to the *a posteriori* error indicator Θ yields optimal convergence and stable effectivity indexes. Notice how the adaptive algorithms improves the efficiency of the method by delivering quality solutions at a lower computational cost, to the point that it is possible to get a better one (in terms of $\mathsf{e}(\boldsymbol{\sigma}, \mathbf{u})$) with approximately only the 0.6% of the degrees of freedom of the last quasi-uniform mesh for the mixed scheme in both cases $k = 0$ and $k = 1$. In addition, we recall from [10, Remark 4.6] that our Galerkin scheme (3.11) satisfies the property $\mathbf{div}\,\boldsymbol{\sigma}_h = \mathbf{P}_h^k(\mathbf{f})$ in Ω, where $\mathbf{P}_h^k$ is the $\mathbf{L}^2(\Omega)$-orthogonal projection onto $\mathbf{M}_h$. In this way, using the fact that $\mathbf{f}$ does not live in $\mathbf{M}_h$, we illustrate the conservation of momentum in an approximate sense by computing the ℓ^∞-norm for $\mathbf{div}\,\boldsymbol{\sigma}_h + \mathbf{P}_h^k(\mathbf{f})$, with $k = 0, 1$. As expected, these values are close to zero.

On the other hand, approximate solutions builded using the $\mathbb{RT}_1 - \mathbf{P}_1$ scheme with $880{,}554$ degrees of freedom ($54{,}955$ triangles), via the indicator Θ, are shown in Figure 6.2. In particular, we observe in the computed magnitude of the velocity a vortex near the corner region of the L-shape domain whereas the pressure exhibits high gradients in the same region. In turn, examples of some adapted meshes for $k = 0$ and $k = 1$ are collected in Figure 6.3. We can observe a clear clustering of elements near the corner region of the contraction as we expected.

Example 3: Adaptivity in a 3D L-shape domain.

To conclude, we replicate the Example 2 in a three-dimensional setting. However, this time we consider the 3D L-shape domain $\Omega := (-0.5, 0.5) \times (0, 0.5) \times (-0.5, 0.5) \setminus (0, 0.5)^3$, and the manufactured exact solutions adopt the form

$$\mathbf{u}(\mathbf{x}) := \begin{pmatrix} \sin(\pi x_1)\cos(\pi x_2)\cos(\pi x_3) \\ -2\,\cos(\pi x_1)\sin(\pi x_2)\cos(\pi x_3) \\ \cos(\pi x_1)\cos(\pi x_2)\sin(\pi x_3) \end{pmatrix},$$

$$p(\mathbf{x}) := \frac{10\,x_3}{(x_1 - 0.02)^2 + (x_3 - 0.02)^2} - p_0 \quad \forall\, \mathbf{x} := (x_1, x_2, x_3) \in \Omega,$$

where $p_0 \in \mathbb{R}$ is a constant chosen in such a way $(p,1)_\Omega = 0$. Similarly, Tables 6.7 and 6.8 along with the Figure 6.4 confirm a disturbed convergence under quasi-uniform refinement and optimal convergence rates when using adaptive refinement guided by the *a posteriori* error estimator Θ.

N	h	$\mathsf{e}(\boldsymbol{\sigma})$	$\mathsf{r}(\boldsymbol{\sigma})$	$\mathsf{e}(\mathbf{u})$	$\mathsf{r}(\mathbf{u})$	$\mathsf{e}(p)$	$\mathsf{r}(p)$	$\mathsf{e}(\nabla\mathbf{u})$	$\mathsf{r}(\nabla\mathbf{u})$	$\mathsf{e}(\boldsymbol{\omega})$	$\mathsf{r}(\boldsymbol{\omega})$	$\mathsf{e}(\boldsymbol{\sigma},\mathbf{u})$	$\mathsf{r}(\boldsymbol{\sigma},\mathbf{u})$	Θ	$\mathsf{eff}(\Theta)$	iter
196	0.373	6.58E+00	–	1.39E-01	–	1.66E+00	–	1.61E+00	–	9.53E-01	–	6.72E+00	–	1.26E+01	0.534	4
792	0.196	3.03E+00	1.110	4.30E-02	1.681	6.63E-01	1.317	8.32E-01	0.949	3.75E-01	1.335	3.07E+00	1.120	6.27E+00	0.490	3
3084	0.098	1.51E+00	1.022	1.66E-02	1.399	2.97E-01	1.181	4.28E-01	0.980	1.67E-01	1.193	1.53E+00	1.027	3.23E+00	0.474	3
12208	0.048	7.79E-01	0.965	7.79E-03	1.100	1.54E-01	0.955	2.35E-01	0.870	7.95E-02	1.075	7.86E-01	0.967	1.71E+00	0.461	3
48626	0.028	3.84E-01	1.023	3.93E-03	0.993	7.16E-02	1.106	1.14E-01	1.042	3.97E-02	1.007	3.88E-01	1.022	8.53E-01	0.455	3
196242	0.014	1.90E-01	1.011	1.91E-04	1.035	3.50E-02	1.027	5.66E-02	1.009	1.97E-02	1.005	1.92E-01	1.011	4.30E-01	0.446	3

Table 6.1: EXAMPLE 1, $\mathbb{RT}_0 - \mathbf{P}_0$ scheme with quasi-uniform refinement.

In turn, some approximated solutions after four mesh refinement steps showing an analogous behavior to its 2-D counterpart are collected in Figure 6.5, whereas snapshots of three meshes via Θ are shown in Figure 6.6.

References

[1] S. AGMON, *Lectures on Elliptic Boundary Value Problems.* Prepared for publication by B. Frank Jones, Jr. with the assistance of George W. Batten, Jr. Revised edition of the 1965 original. AMS Chelsea Publishing, Providence, RI, 2010.

[2] M. AINSWORTH AND J.T. ODEN, *A unified approach to a posteriori error estimation based on element residual methods.* Numer. Math. 65 (1993), no. 1, 23–50.

[3] M. AINSWORTH AND J.T. ODEN, *A posteriori error estimators for the Stokes and Oseen equations.* SIAM J. Numer. Anal. 34 (1997), no. 1, 228–245.

[4] M. AINSWORTH AND J.T. ODEN, *A Posterori Error Estimation in Finite Element Analysis.* Pure and Applied Mathematics (New York). Wiley-Interscience [John Wiley & Sons], New York, 2000.

[5] A. ALONSO, *Error estimators for a mixed method.* Numer. Math. 74 (1996), no. 4, 385–395

[6] A. ALLENDES, E. OTAROLA, A. J. SALGADO, *A posteriori error estimates for the stationary NavierStokes equations with Dirac measures.* SIAM J. Sci. Comput. 42 (2020), no. 3, A1860–A1884.

[7] G.A. BENAVIDES, S. CAUCAO, G.N. GATICA AND A.A. HOPPER, *A Banach spaces-based analysis of a new mixed-primal finite element method for a coupled flow-transport problem.* Comput. Methods Appl. Mech. Engrg. 371 (2020), 113285.

N	h	$\mathsf{e}(\boldsymbol{\sigma})$	$\mathsf{r}(\boldsymbol{\sigma})$	$\mathsf{e}(\mathbf{u})$	$\mathsf{r}(\mathbf{u})$	$\mathsf{e}(p)$	$\mathsf{r}(p)$	$\mathsf{e}(\nabla\mathbf{u})$	$\mathsf{r}(\nabla\mathbf{u})$	$\mathsf{e}(\boldsymbol{\omega})$	$\mathsf{r}(\boldsymbol{\omega})$	$\mathsf{e}(\boldsymbol{\sigma},\mathbf{u})$	$\mathsf{r}(\boldsymbol{\sigma},\mathbf{u})$	Θ	$\mathsf{eff}(\Theta)$	iter
608	0.3727	8.11E-01	–	1.50E-02	–	1.44E-01	–	2.45E-01	–	1.23E-01	–	8.26E-01	–	2.58E+00	0.321	3
2496	0.1964	1.70E-01	2.211	3.54E-03	2.044	3.22E-02	2.123	5.48E-02	2.117	2.46E-02	2.285	1.74E-01	2.208	5.67E-01	0.306	3
9792	0.0978	4.34E-02	1.997	8.36E-04	2.112	8.48E-03	1.953	1.45E-02	1.945	6.14E-03	2.028	4.43E-02	2.000	1.48E-01	0.299	3
38912	0.0481	1.12E-02	1.958	2.09E-04	2.008	2.21E-03	1.946	3.82E-03	1.933	1.60E-03	1.948	1.15E-02	1.959	3.94E-02	0.291	3
155296	0.0279	2.76E-03	2.029	5.69E-05	1.882	5.32E-04	2.060	9.26E-04	2.049	3.85E-04	2.058	2.82E-03	2.026	9.95E-03	0.283	3
627360	0.0142	6.74E-04	2.021	1.38E-05	2.028	1.30E-04	2.017	2.26E-04	2.019	9.33E-05	2.031	6.88E-04	2.021	2.55E-03	0.269	3

Table 6.2: Example 1, $\mathbb{RT}_1 - \mathbf{P}_1$ scheme with quasi-uniform refinement.

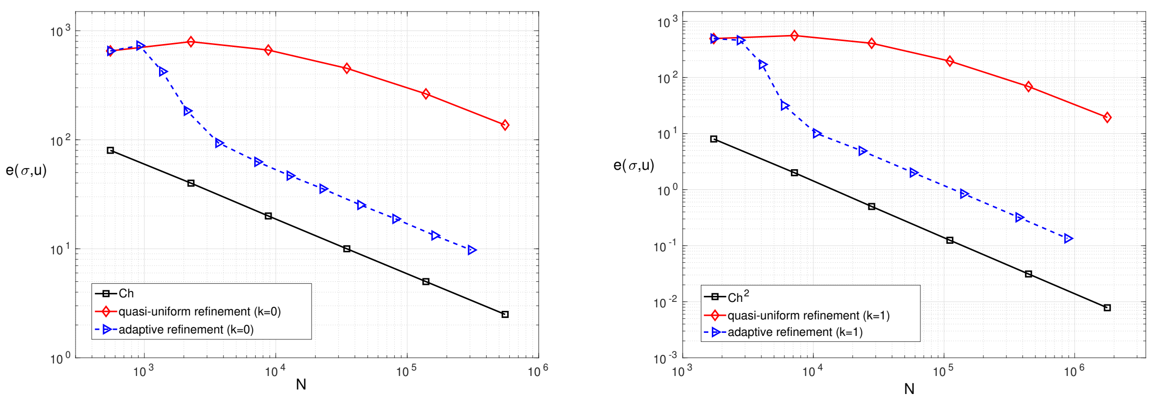

Figure 6.1: Example 2, Log-log plot of $\mathsf{e}(\boldsymbol{\sigma},\mathbf{u})$ vs. N for quasi-uniform/adaptive refinements for $k=0$ and $k=1$ (left and right plots, respectively).

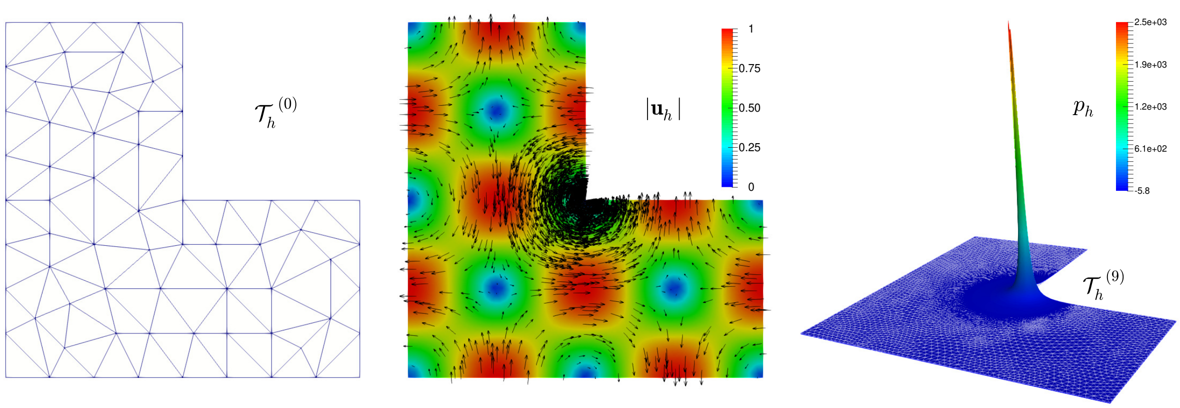

Figure 6.2: Example 2, initial mesh, computed magnitude of the velocity, and pressure field.

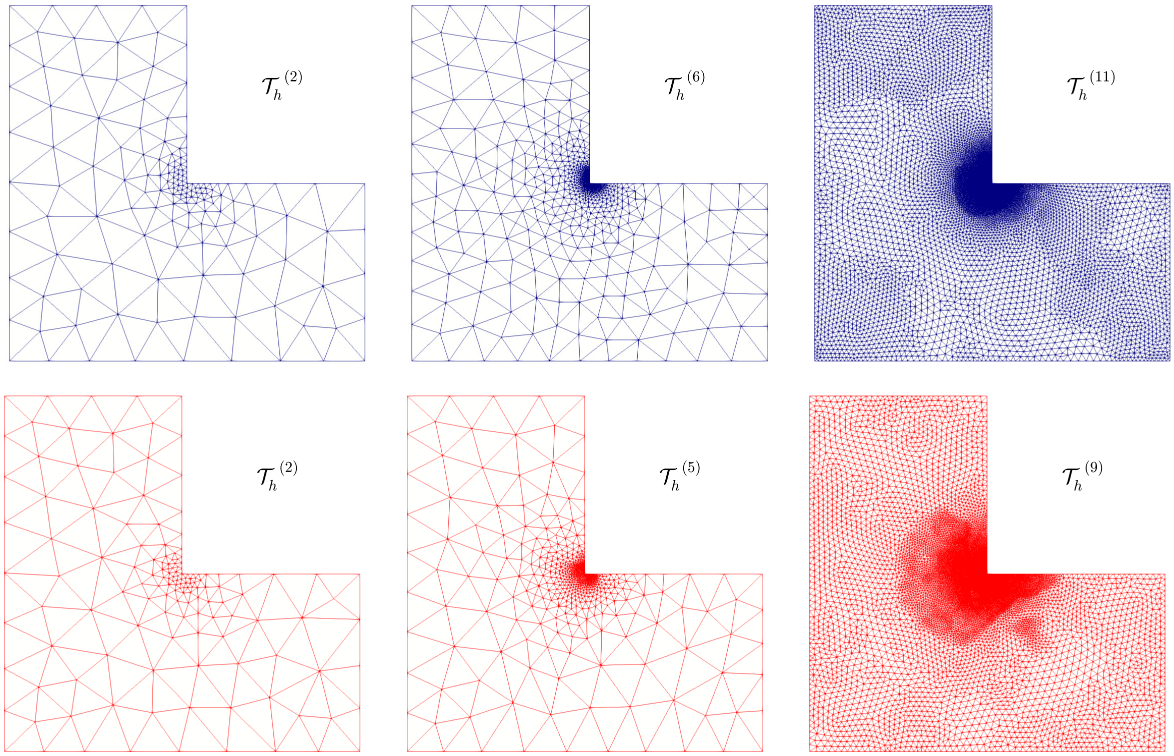

Figure 6.3: Example 2, three snapshots of adapted meshes according to the indicator Θ for $k = 0$ and $k = 1$ (top and bottom plots, respectively).

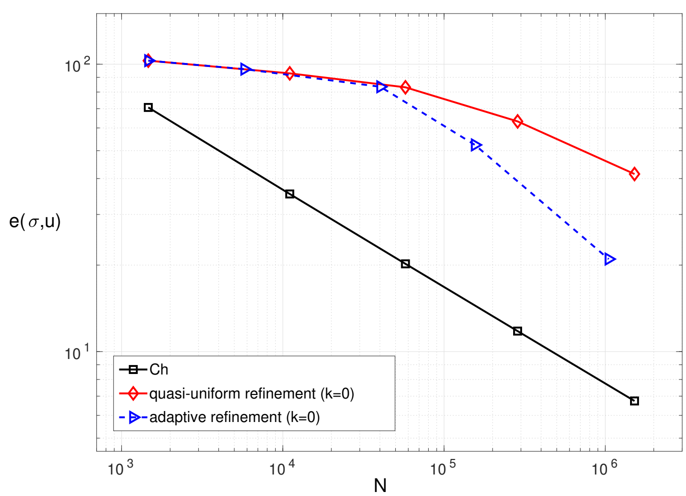

Figure 6.4: Example 3, Log-log plot of $\mathsf{e}(\boldsymbol{\sigma}, \mathbf{u})$ vs. N for quasi-uniform/adaptive refinements for $k = 0$.

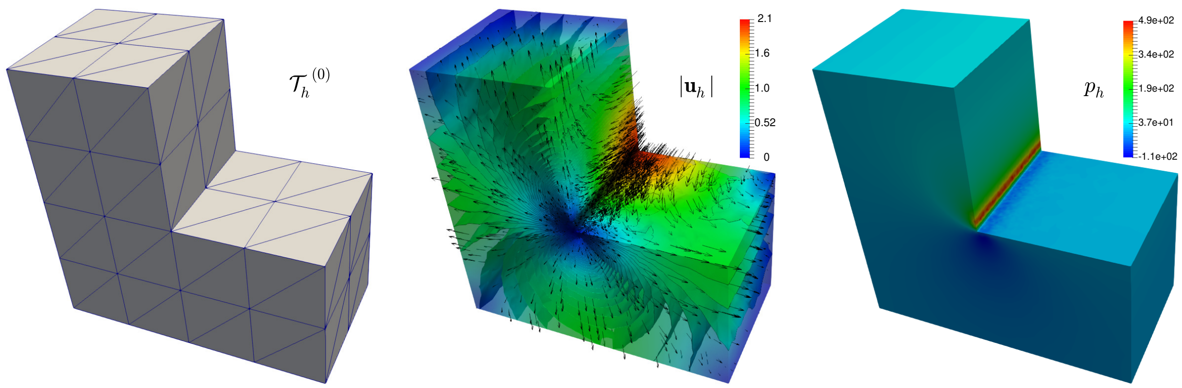

Figure 6.5: Example 3, initial mesh, computed magnitude of the velocity, and pressure field.

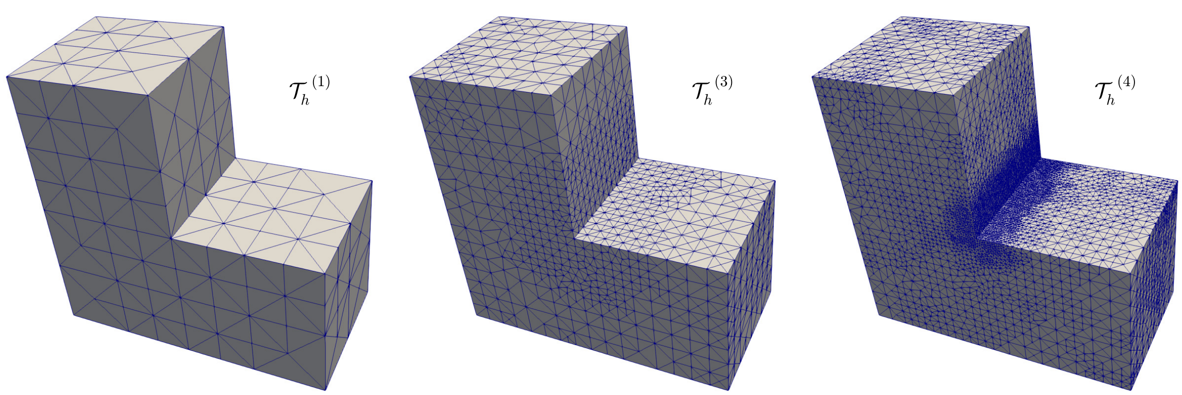

Figure 6.6: Example 3, three snapshots of adapted meshes according to the indicator Θ for $k = 0$.

N	h	$\mathsf{e}(\boldsymbol{\sigma})$	$\mathsf{r}(\boldsymbol{\sigma})$	$\mathsf{e}(\mathbf{u})$	$\mathsf{r}(\mathbf{u})$	$\mathsf{e}(p)$	$\mathsf{r}(p)$	$\mathsf{e}(\nabla\mathbf{u})$	$\mathsf{r}(\nabla\mathbf{u})$
552	0.400	6.48E+02	–	5.72E+00	–	3.78E+01	–	4.89E+01	–
2264	0.190	7.91E+02	–	3.51E+00	0.693	3.87E+01	–	4.31E+01	0.180
8778	0.103	6.63E+02	0.260	2.34E+00	0.600	2.74E+01	0.508	3.84E+01	0.169
34726	0.051	4.51E+02	0.559	1.04E+00	1.170	1.87E+01	0.556	2.64E+01	0.543
138722	0.027	2.63E+02	0.778	3.94E-01	1.407	1.03E+01	0.863	1.59E+01	0.734
555584	0.014	1.36E+02	0.948	1.15E-01	1.773	5.15E+00	0.998	8.29E+00	0.939

$\mathsf{e}(\boldsymbol{\omega})$	$\mathsf{r}(\boldsymbol{\omega})$	$\mathsf{e}(\boldsymbol{\sigma},\mathbf{u})$	$\mathsf{r}(\boldsymbol{\sigma},\mathbf{u})$	Θ	$\mathsf{eff}(\Theta)$	$\lVert\mathbf{div}\,\boldsymbol{\sigma}_h + \mathbf{P}_h^0(\mathbf{f})\rVert_{\ell^\infty}$	iter
2.35E+01	–	6.53E+02	–	8.37E+02	0.780	4.55E-13	5
1.67E+01	0.483	7.94E+02	–	9.45E+02	0.840	9.09E-13	4
1.83E+01	–	6.65E+02	0.261	8.08E+02	0.823	7.28E-12	4
1.19E+01	0.632	4.52E+02	0.561	5.51E+02	0.820	1.09E-11	4
7.06E+00	0.748	2.63E+02	0.780	3.27E+02	0.806	5.09E-11	3
3.37E+00	1.066	1.37E+02	0.949	1.70E+02	0.802	1.16E-10	3

Table 6.3: Example 2, $\mathbb{RT}_0 - \mathbf{P}_0$ scheme with quasi-uniform refinement.

[8] D. Braess and R. Verfürth, *A posteriori error estimators for the Raviart-Thomas element*. SIAM J. Numer. Anal. 33 (1996), no. 6, 2431–2444.

[9] F. Brezzi and M. Fortin, *Mixed and Hybrid Finite Element Methods*. Springer Series in Computational Mathematics, 15. Springer–Verlag, New York, 1991.

[10] J. Camaño, C. García, and R. Oyarzúa, *Analysis of a conservative mixed-FEM for the stationary Navier–Stokes problem*. Preprint 2018-25, Centro de Investigación en Ingeniería Matemática ($\mathrm{CI^2MA}$), Universidad de Concepción, Concepción, Chile, (2018).

[11] J. Camaño, C. García and R. Oyarzúa, *Analysis of a new mixed-FEM for stationary incompressible magneto-hydrodynamics*. Preprint 2020-13, Centro de Investigación en Ingeniería Matemática ($\mathrm{CI^2MA}$), Universidad de Concepción, Concepción, Chile, (2020).

[12] J. Camaño, G.N. Gatica, R. Oyarzúa and R. Ruiz-Baier, *An augmented stress-based mixed finite element method for the steady state Navier-Stokes equations with nonlinear viscosity*. Numer. Methods Partial Differential Equations 33 (2017), no. 5, 1692–1725.

[13] C. Carstensen, *A posteriori error estimate for the mixed finite element method*. Math. Comp. 66 (1997), no. 218, 465–476.

[14] C. Carstensen and G. Dolzmann, *A posteriori error estimates for mixed FEM in elasticity*. Numer. Math. 81 (1998), no. 2, 187–209.

[15] S. Caucao, D. Mora, and R. Oyarzúa, *A priori and a posteriori error analysis of a pseudostress-based mixed formulation of the Stokes problem with varying density*. IMA J. Numer. Anal. 36 (2016), no. 2, 947–983.

[16] S. Caucao, R. Oyarzúa and S. Villa-Fuentes, *A new mixed-FEM for steady-state natural convection models allowing conservation of momentum and thermal energy*. Preprint 2019-41, Centro de Investigación en Ingeniería Matemática ($\mathrm{CI^2MA}$), Universidad de Concepción, Concepción, Chile, (2019).

N	h	$\mathsf{e}(\boldsymbol{\sigma})$	$\mathsf{r}(\boldsymbol{\sigma})$	$\mathsf{e}(\mathbf{u})$	$\mathsf{r}(\mathbf{u})$	$\mathsf{e}(p)$	$\mathsf{r}(p)$	$\mathsf{e}(\nabla\mathbf{u})$	$\mathsf{r}(\nabla\mathbf{u})$
1728	0.400	4.92E+02	–	2.57E+00	–	2.38E+01	–	3.43E+01	–
7168	0.190	5.59E+02	–	1.63E+00	0.637	1.95E+01	0.283	3.15E+01	0.121
27936	0.103	4.07E+02	0.464	5.84E-01	1.512	1.12E+01	0.813	1.78E+01	0.842
110816	0.051	1.96E+02	1.064	1.69E-01	1.803	5.38E+00	1.064	8.51E+00	1.068
443296	0.027	6.89E+01	1.506	4.00E-02	2.078	1.74E+00	1.627	3.07E+00	1.470
1776640	0.014	1.94E+01	1.827	5.92E-03	2.751	4.90E-01	1.827	8.48E-01	1.853

$\mathsf{e}(\boldsymbol{\omega})$	$\mathsf{r}(\boldsymbol{\omega})$	$\mathsf{e}(\boldsymbol{\sigma},\mathbf{u})$	$\mathsf{r}(\boldsymbol{\sigma},\mathbf{u})$	Θ	$\mathsf{eff}(\Theta)$	$\\|\mathbf{div}\,\boldsymbol{\sigma}_h + \mathbf{P}_h^1(\mathbf{f})\\|_{\ell^\infty}$	iter
1.62E+01	–	4.95E+02	–	8.42E+02	0.588	9.38E-13	4
1.55E+01	0.063	5.60E+02	–	7.56E+02	0.741	3.64E-12	4
8.95E+00	0.805	4.08E+02	0.466	5.46E+02	0.748	1.18E-11	3
3.95E+00	1.190	1.96E+02	1.065	2.64E+02	0.742	8.73E-11	3
1.38E+00	1.519	6.90E+01	1.506	9.41E+01	0.733	1.46E-10	3
3.62E-01	1.924	1.94E+01	1.827	2.64E+01	0.734	2.91E-10	3

Table 6.4: EXAMPLE 2, $\mathbb{RT}_1 - \mathbf{P}_1$ scheme with quasi-uniform refinement.

N	$\mathsf{e}(\boldsymbol{\sigma})$	$\mathsf{r}(\boldsymbol{\sigma})$	$\mathsf{e}(\mathbf{u})$	$\mathsf{r}(\mathbf{u})$	$\mathsf{e}(p)$	$\mathsf{r}(p)$	$\mathsf{e}(\nabla\mathbf{u})$	$\mathsf{r}(\nabla\mathbf{u})$
552	6.48E+02	–	5.72E+00	–	3.78E+01	–	4.89E+01	–
920	7.29E+02	–	2.21E+00	3.722	3.10E+01	0.773	3.57E+01	1.230
1370	4.22E+02	2.741	7.42E-01	5.486	1.55E+01	3.475	2.21E+01	2.412
2110	1.84E+02	3.843	2.63E-01	4.808	6.77E+00	3.846	1.01E+01	3.629
3666	9.33E+01	2.462	2.54E-01	0.123	3.43E+00	2.458	5.38E+00	2.277
7256	6.25E+01	1.175	2.53E-01	0.016	2.32E+00	1.146	3.69E+00	1.109
12786	4.67E+01	1.027	1.84E-01	1.114	1.71E+00	1.076	2.73E+00	1.058
22746	3.54E+01	0.961	1.36E-01	1.041	1.29E+00	0.988	2.06E+00	0.978
44082	2.51E+01	1.035	9.48E-02	1.102	9.12E-01	1.040	1.47E+00	1.024
81474	1.88E+01	0.955	6.68E-02	1.138	6.77E-01	0.969	1.09E+00	0.973
161434	1.32E+01	1.024	4.67E-02	1.051	4.79E-01	1.013	7.71E-01	1.011
306256	9.72E+00	0.959	3.19E-02	1.191	3.51E-01	0.977	5.63E-01	0.983

$\mathsf{e}(\boldsymbol{\omega})$	$\mathsf{r}(\boldsymbol{\omega})$	$\mathsf{e}(\boldsymbol{\sigma},\mathbf{u})$	$\mathsf{r}(\boldsymbol{\sigma},\mathbf{u})$	Θ	$\mathsf{eff}(\Theta)$	$\\|\mathbf{div}\,\boldsymbol{\sigma}_h + \mathbf{P}_h^0(\mathbf{f})\\|_{\ell^\infty}$	iter
2.35E+01	–	6.53E+02	–	8.37E+02	0.780	4.55E-13	5
1.44E+01	1.913	7.31E+02	–	8.53E+02	0.858	3.64E-12	4
8.95E+00	2.394	4.23E+02	2.748	5.03E+02	0.841	1.82E-11	4
3.75E+00	4.031	1.85E+02	3.844	2.24E+02	0.825	8.73E-11	3
1.86E+00	2.532	9.36E+01	2.458	1.16E+02	0.809	3.49E-10	3
1.29E+00	1.066	6.27E+01	1.172	7.80E+01	0.804	1.05E-09	3
9.39E-01	1.136	4.69E+01	1.027	5.83E+01	0.804	1.26E-09	3
7.07E-01	0.986	3.56E+01	0.961	4.43E+01	0.803	1.91E-09	3
5.05E-01	1.014	2.52E+01	1.035	3.15E+01	0.801	2.66E-09	3
3.70E-01	1.019	1.88E+01	0.956	2.35E+01	0.800	4.57E-09	3
2.62E-01	1.008	1.33E+01	1.024	1.66E+01	0.796	5.15E-09	3
1.89E-01	1.022	9.75E+00	0.960	1.23E+01	0.795	9.30E-09	3

Table 6.5: EXAMPLE 2, $\mathbb{RT}_0 - \mathbf{P}_0$ scheme with adaptive refinement via Θ.

N	$\mathsf{e}(\boldsymbol{\sigma})$	$\mathsf{r}(\boldsymbol{\sigma})$	$\mathsf{e}(\mathbf{u})$	$\mathsf{r}(\mathbf{u})$	$\mathsf{e}(p)$	$\mathsf{r}(p)$	$\mathsf{e}(\nabla\mathbf{u})$	$\mathsf{r}(\nabla\mathbf{u})$
1728	4.92E+02	–	2.57E+00	–	2.38E+01	–	3.43E+01	–
2742	4.61E+02	0.283	9.12E-01	4.491	1.19E+01	3.020	2.22E+01	1.889
4052	1.71E+02	5.076	1.36E-01	9.732	4.36E+00	5.122	6.91E+00	5.972
5974	3.16E+01	8.706	3.24E-02	7.413	7.54E-01	9.042	1.25E+00	8.795
10506	1.01E+01	4.051	3.21E-02	0.026	2.79E-01	3.522	4.71E-01	3.465
23492	4.89E+00	1.794	2.63E-02	0.493	1.30E-01	1.903	2.17E-01	1.927
57828	2.01E+00	1.974	4.43E-03	3.960	5.51E-02	1.902	9.24E-02	1.898
140672	8.40E-01	1.962	4.06E-03	0.194	2.22E-02	2.043	3.77E-02	2.018
372550	3.20E-01	1.985	5.55E-04	4.088	8.69E-03	1.928	1.45E-02	1.955
880554	1.34E-01	2.017	4.91E-04	0.284	3.48E-03	2.128	5.87E-03	2.107

$\mathsf{e}(\boldsymbol{\omega})$	$\mathsf{r}(\boldsymbol{\omega})$	$\mathsf{e}(\boldsymbol{\sigma},\mathbf{u})$	$\mathsf{r}(\boldsymbol{\sigma},\mathbf{u})$	Θ	$\mathsf{eff}(\Theta)$	$\\|\mathbf{div}\,\boldsymbol{\sigma}_h + \mathbf{P}_h^1(\mathbf{f})\\|_{\ell^\infty}$	iter
1.62E+01	–	4.95E+02	–	8.42E+02	0.588	9.38E-13	4
1.16E+01	1.457	4.62E+02	0.297	5.89E+02	0.784	7.28E-12	4
3.01E+00	6.901	1.71E+02	5.082	2.17E+02	0.789	2.55E-11	3
4.79E-01	9.466	3.16E+01	8.705	4.05E+01	0.781	1.75E-10	3
1.84E-01	3.386	1.01E+01	4.043	1.37E+01	0.738	9.60E-10	3
8.64E-02	1.879	4.92E+00	1.789	6.58E+00	0.747	2.15E-09	3
3.54E-02	1.982	2.01E+00	1.981	2.69E+00	0.748	6.81E-09	3
1.51E-02	1.921	8.44E-01	1.956	1.15E+00	0.735	9.34E-09	3
5.53E-03	2.057	3.20E-01	1.991	4.28E-01	0.748	1.14E-08	3
2.30E-03	2.039	1.35E-01	2.013	1.85E-01	0.727	2.21E-08	3

Table 6.6: EXAMPLE 2, $\mathbb{RT}_1 - \mathbf{P}_1$ scheme with adaptive refinement via Θ.

N	h	$\mathsf{e}(\boldsymbol{\sigma})$	$\mathsf{r}(\boldsymbol{\sigma})$	$\mathsf{e}(\mathbf{u})$	$\mathsf{r}(\mathbf{u})$	$\mathsf{e}(p)$	$\mathsf{r}(p)$	$\mathsf{e}(\nabla\mathbf{u})$	$\mathsf{r}(\nabla\mathbf{u})$
1464	0.354	1.02E+02	–	1.03E+00	–	9.34E+00	–	7.85E+00	–
11040	0.177	9.23E+01	0.147	6.52E-01	0.684	7.93E+00	0.243	6.64E+00	0.249
57624	0.101	8.27E+01	0.199	4.30E-01	0.757	6.37E+00	0.396	5.77E+00	0.255
285984	0.059	6.30E+01	0.509	2.32E-01	1.154	4.24E+00	0.762	4.39E+00	0.511
1518804	0.034	4.14E+01	0.756	1.11E-01	1.317	2.49E+00	0.956	3.02E+00	0.671

$\mathsf{e}(\boldsymbol{\omega})$	$\mathsf{r}(\boldsymbol{\omega})$	$\mathsf{e}(\boldsymbol{\sigma},\mathbf{u})$	$\mathsf{r}(\boldsymbol{\sigma},\mathbf{u})$	Θ	$\mathsf{eff}(\Theta)$	iter
4.52E+00	–	1.03E+02	–	1.16E+02	0.885	4
3.49E+00	0.387	9.29E+01	0.151	1.01E+02	0.922	4
2.85E+00	0.365	8.31E+01	0.203	8.87E+01	0.936	4
2.03E+00	0.636	6.32E+01	0.511	6.71E+01	0.943	3
1.35E+00	0.738	4.15E+01	0.757	4.40E+01	0.943	5

Table 6.7: EXAMPLE 3, $\mathbb{RT}_0 - \mathbf{P}_0$ scheme with quasi-uniform refinement.

N	e($\boldsymbol{\sigma}$)	r($\boldsymbol{\sigma}$)	e($\mathbf{u}$)	r($\mathbf{u}$)	e(p)	r(p)	e($\nabla\mathbf{u}$)	r($\nabla\mathbf{u}$)
1464	1.02E+02	–	1.03E+00	–	9.34E+00	–	7.85E+00	–
5784	9.54E+01	0.143	7.29E-01	0.762	8.26E+00	0.266	6.85E+00	0.298
40293	8.30E+01	0.214	4.22E-01	0.844	5.92E+00	0.516	5.67E+00	0.292
155496	5.22E+01	1.031	1.69E-01	2.034	3.15E+00	1.399	3.68E+00	0.960
1050117	2.09E+01	1.435	4.41E-02	2.108	1.15E+00	1.582	1.58E+00	1.330

e($\boldsymbol{\omega}$)	r($\boldsymbol{\omega}$)	e($\boldsymbol{\sigma},\mathbf{u}$)	r($\boldsymbol{\sigma},\mathbf{u}$)	Θ	eff(Θ)	iter
4.52E+00	–	1.03E+02	–	1.16E+02	0.885	4
3.55E+00	0.532	9.61E+01	0.149	1.04E+02	0.921	4
2.62E+00	0.468	8.34E+01	0.218	8.87E+01	0.940	4
1.59E+00	1.111	5.24E+01	1.035	5.56E+01	0.941	3
5.80E-01	1.581	2.10E+01	1.436	2.27E+01	0.925	3

Table 6.8: Example 3, $\mathbb{RT}_0 - \mathbf{P}_0$ scheme with adaptive refinement via Θ.

[17] S. Caucao and I. Yotov, *A Banach space mixed formulation for the unsteady Brinkman-Forchheimer equations.* IMA J. Numer. Anal. https://doi.org/10.1093/imanum/draa035.

[18] Ph. Clément, *Approximation by finite element functions using local regularisation.* R.A.I.R.O. Analyse Numérique 9, N R2 (1975) 77–84

[19] E. Colmenares, G.N. Gatica and S. Moraga, *A Banach spaces-based analysis of a new fully-mixed finite element method for the Boussinesq problem.* ESAIM Math. Model. Numer. Anal. 54 (2020), no. 5, 1525–1568.

[20] E. Colmenares, G.N. Gatica, and R. Oyarza, *A posteriori error analysis of an augmented mixedprimal formulation for the stationary Boussinesq model.* Calcolo 54 (2017), no. 3, 1055–1095.

[21] C. Domínguez, G.N. Gatica, and S. Meddahi, *A posteriori error analysis of a fully-mixed finite element method for a two-dimensional fluid-solid interaction problem.* J. Comput. Math. 33 (2015), no. 6, 606–641.

[22] A. Ern and J.-L.Guermond, *Theory and Practice of Finite Elements.* Applied Mathematical Sciences, 159. Springer–Verlag, New York, 2004.

[23] M. Farhloul, S. Nicaise and L. Paquet, *A priori and a posteriori error estimations for the dual mixed finite element method of the Navier-Stokes problem.* Numer. Methods Partial Differential Equations 25 (2009), no. 4, 843–869.

[24] G.N. Gatica, *A note on stable Helmholtz decompositions in 3D.* Appl. Anal. 99 (2020), no. 7, 1110–1121.

[25] G.N. Gatica, *A Simple Introduction to the Mixed Finite Element Method. Theory and applications.* SpringerBriefs in Mathematics. Springer, Cham, 2014.

[26] G.N. Gatica, L.F. Gatica, and F.A. Sequeira, *A priori and a posteriori error analyses of a pseudostress-based mixed formulation for linear elasticity.* Comput. Math. Appl. 71 (2016), no. 2, 585–614.

[27] G.N. Gatica and M. Maischak, *A posteriori error estimates for the mixed finite element method with Lagrange multipliers.* Numer. Methods Partial Differential Equations 21 (2005), no. 3, 421–450.

[28] G.N. Gatica, A. Márquez and M.A. Sánchez, *Analysis of a velocity-pressure-pseudostress formulation for the stationary Stokes equations.* Comput. Methods Appl. Mech. Engrg. 199 (2010), no. 17-20, 1064–1079.

[29] G.N. Gatica, R. Ruiz-Baier and G. Tierra, *A posteriori error analysis of an augmented mixed method for the Navier-Stokes equations with nonlinear viscosity.* Comput. Math. Appl. 72 (2016), no. 9, 2289–2310.

[30] V. Girault and P.-A. Raviart, *Finite Element Methods for Navier–Stokes Equations. Theory and Algorithms.* Springer Series in Computational Mathematics, 5. Springer–Verlag, Berlin, 1986.

[31] P. Grisvard, *Elliptic Problems in Nonsmooth Domains.* Classics in Applied Mathematics, 69. Society for Industrial and Applied Mathematics (SIAM), Philadelphia, PA, 2011.

[32] F. Hecht, *New development in freefem++.* J. Numer. Math. 20 (2012), no. 3-4, 251–265.

[33] F. Hecht, *Freefem++.* Third Edition, Version 3.58-1. Laboratoire Jacques-Louis Lions, Université Pierre et Marie Curie, Paris, 2018. [available in `http://www.freefem.org/ff++`].

[34] R.H.W. Hoppe and B.I. Wohlmuth, *A comparison of a posteriori error estimators for mixed finite element discretizations by Raviart-Thomas elements.* Math. Comp. 68 (1999), no. 228, 1347–1378.

[35] G. Kanschat and D. Schötzau, *Energy norm a posteriori error estimation for divergence-free discontinuous Galerkin approximations of the Navier–Stokes equations* Internat. J. Numer. Methods Fluids 57 (2008), no. 9, 1093–1113.

[36] M. Lonsing and R. Verfürth, *A posteriori error estimators for mixed finite element methods in linear elasticity.* Numer. Math. 97 (2004), no. 4, 757–778.

[37] C. Lovadina and R. Stenberg, *Energy norm a posteriori error estimates for mixed finite element methods.* Math. Comp. 75 (2006), no. 256, 1659–1674.

[38] J.T. Oden, W. Wu and M. Ainsworth. *An a posteriori error estimate for finite element approximations of the Navier-Stokes equations.* Comput. Methods Appl. Mech. Engrg. 111 (1994), no. 1-2, 185–202.

[39] R. Oyarzúa and M. Serón. *A Divergence-Conforming DG-Mixed Finite Element Method for the Stationary Boussinesq Problem.* J. Sci. Comput. 85 (2020), no. 1, 14.

[40] S. Repin, S. Sauter and A. Smolianski, *Two-sided a posteriori error estimates for mixed formulations of elliptic problems.* SIAM J. Numer. Anal. 45 (2007), no. 3, 928–945.

[41] R. Verfürth, *A posteriori error estimators and adaptive mesh-refinement techniques for the Navier Stokes equations.* Incompressible computational fluid dynamics: trends and advances, 447–475, Cambridge Univ. Press, Cambridge, 2008.

[42] R. Verfürth, *A posteriori error estimates for non-linear problems. Finite element discretizations of elliptic equations*. Math. Comp. 62 (1994), no. 206, 445–475.

[43] R. Verfürth, *A posteriori error estimation and adaptive mesh-refinement thecniques*. J. Comput. Appl. Math. 50 (1994), no. 1–3, 67–83.

[44] R. Verfürth, *A Review of A-Posteriori Error Estimation and Adaptive Mesh-Refinement Techniques*. Wiley Teubner, Chichester, 1996.